

This is an Open Access document downloaded from ORCA, Cardiff University's institutional repository: <https://orca.cardiff.ac.uk/id/eprint/162715/>

This is the author's version of a work that was submitted to / accepted for publication.

Citation for final published version:

Nederbragt, Alexandra J. 2023. The effect of seawater carbonate chemistry on the stable isotope composition of *Cibicidoides wuellerstorfi* and other *Cibicidoides* species. *Paleoceanography and Paleoclimatology* 38 (9), e2023PA004667. 10.1029/2023PA004667

Publishers page: <http://dx.doi.org/10.1029/2023PA004667>

Please note:

Changes made as a result of publishing processes such as copy-editing, formatting and page numbers may not be reflected in this version. For the definitive version of this publication, please refer to the published source. You are advised to consult the publisher's version if you wish to cite this paper.

This version is being made available in accordance with publisher policies. See <http://orca.cf.ac.uk/policies.html> for usage policies. Copyright and moral rights for publications made available in ORCA are retained by the copyright holders.



1 **The Effect of Seawater Carbonate Chemistry on the Stable Isotope Composition of**
2 ***Cibicidoides wuellerstorfi* and Other *Cibicidoides* Species**

3
4 **Alexandra J. Nederbragt¹**

5 ¹School of Earth and Environmental Sciences

6 Cardiff University

7 Main Building, Park Place

8 Cardiff CF10 3AT, Wales, U.K.

9
10 Alexandra Nederbragt (NederbragtA@cardiff.ac.uk)

11
12
13
14
15 **Key Points:**

- 16 • The offset between the measured and expected $\delta^{13}\text{C}$ and $\delta^{18}\text{O}$ of *Cibicidoides*
17 *wuellerstorfi* correlates with seawater carbonate chemistry
- 18 • Negative $\Delta^{13}\text{C}$ occur mainly in the deep Atlantic due to a combination of low
19 temperature, under-saturation, and low to intermediate [DIC]
20

21 Abstract

22 The $\delta^{13}\text{C}$ composition of *Cibicidoides wuellerstorfi* and other *Cibicidoides* spp is an important
 23 tool to reconstruct past changes in the deep ocean carbon cycle. The species are expected to
 24 match the $\delta^{13}\text{C}$ of ambient dissolved inorganic carbon (DIC), although it has been recognised
 25 that substantial offsets can occur. Here I present a compilation of modern $\delta^{13}\text{C}$ and $\delta^{18}\text{O}$ data for
 26 named *Cibicidoides* species in combination with fully resolved carbonate chemistry at each core
 27 location. The data show for *C. wuellerstorfi* that the offset from the expected value in both
 28 carbon ($\Delta^{13}\text{C}$) and oxygen ($\Delta^{18}\text{O}$) is correlated with seawater carbonate chemistry. The result is
 29 comparable to, but not identical with, published culture experiments in which marine organisms
 30 were grown under variable pH-conditions. Overall, $\Delta^{13}\text{C}$ in *C. wuellerstorfi* correlates positively
 31 with carbonate saturation, [DIC], and temperature. The three variables together explain 47.1% of
 32 the variation in $\Delta^{13}\text{C}$. The trend for $\Delta^{18}\text{O}$ is similar, except that the effect of temperature has been
 33 removed through correction with a published $\delta^{18}\text{O}$ -temperature equation. Up to 35% of the
 34 remaining variation in $\Delta^{18}\text{O}$ can be explained by ambient carbonate chemistry. Data for other
 35 named *Cibicidoides* species are broadly similar, but are too sparse for a detailed analysis. The
 36 results indicate that strongly negative $\Delta^{13}\text{C}$ occurs predominantly in the deep Atlantic in response
 37 to a combination of low [DIC], low temperature, and undersaturation within the lysocline.
 38 Implications for paleoceanographic reconstructions are discussed.

39

40 1 Introduction

41 The stable carbon isotope composition of dissolved inorganic carbon (DIC) in the deep
 42 ocean provides a tracer for ocean circulation and the age of bottom water masses. The $\delta^{13}\text{C}$ of
 43 DIC ($\delta^{13}\text{C}_{\text{DIC}}$) in deep water masses initially reflects ocean chemistry at the source location but
 44 decreases progressively through remineralisation of sinking organic matter. Epifaunal benthic
 45 foraminifera like *Cibicidoides* species are considered to record the $\delta^{13}\text{C}$ composition of ambient
 46 deep water faithfully and are therefore the preferred material to reconstruct past changes in ocean
 47 circulation (Duplessy et al., 1984; Hodell et al., 2003; Peterson et al., 2014; Schmittner et al.,
 48 2017).

49 However, it has been recognised that the $\delta^{13}\text{C}$ of *Cibicidoides* spp. ($\delta^{13}\text{C}_{\text{Cib}}$) can be
 50 substantially lower than that of ambient DIC. The effect has been linked to the presence of
 51 phytodetritus on the sea floor in areas with seasonally high rain rates of organic matter
 52 (Mackensen et al., 1993; Mackensen et al., 2001). However, a subsequent compilation of global
 53 $\delta^{13}\text{C}_{\text{Cib}}$ data shows features that are inconsistent with this explanation. Schmittner et al. (2017)
 54 show that the offset between $\delta^{13}\text{C}_{\text{Cib}}$ and ambient DIC correlates with water depth, with negative
 55 offsets occurring preferentially in the deep ocean. In contrast, phytodetritus should be more
 56 abundant in shallow water, since the flux of organic matter decreases exponentially with
 57 increasing water depth (Armstrong et al., 2002; Martin et al., 1987). Furthermore, the most
 58 depleted $\delta^{13}\text{C}_{\text{Cib}}$ values are essentially restricted to the deep Atlantic Ocean; such values are very
 59 rare or absent in the Indian and Pacific Oceans (Schmittner et al., 2017) irrespective of water
 60 depth or levels of productivity in the overlying surface waters.

61 The aim of this paper is to determine if exceptionally low $\delta^{13}\text{C}_{\text{Cib}}$ can be explained by the
 62 carbonate chemistry of ambient water instead. Schmittner et al. (2017) found a weak but
 63 significant correlation with carbonate ion concentration ($[\text{CO}_3^{2-}]$). The authors estimated $[\text{CO}_3^{2-}]$

64 as the difference between Total Alkalinity (TA) and DIC concentrations, which is a convenient
 65 approximation but not accurate enough for any detailed analysis (Broecker & Peng, 1982; Yu et
 66 al., 2016). Yet there is evidence that carbonate chemistry affects the chemical composition of
 67 foraminifera. The trace metal composition of benthic foraminifera, including *Cibicidoides*, is
 68 sensitive to the carbonate saturation state of ambient sea water (Elderfield et al., 2006; Yu et al.,
 69 2007). Both $\delta^{13}\text{C}$ and $\delta^{18}\text{O}$ of cultured planktonic foraminifera changed substantially when
 70 ambient $[\text{CO}_3^{2-}]$ was modified (Spero et al., 1997). Additionally, changes in carbonate chemistry
 71 could induce vital effects if the habitat of benthic foraminifera is dependent on ambient
 72 conditions. Specifically, Wollenburg et al. (2018) found that *Cibicidoides pachyderma* switches
 73 between epifaunal and infaunal habitats depending on ambient pH.

74 To determine if there is a consistent correlation between the stable isotope composition of
 75 *Cibicidoides* and ambient deep water carbonate chemistry, I therefore compiled published $\delta^{13}\text{C}$
 76 and $\delta^{18}\text{O}$ data for named *Cibicidoides* species in conjunction with fully resolved carbonate
 77 chemistry at each core location. The main focus is on *Cibicidoides wuellerstorfi* (Schwager), as
 78 this is the species that has been analysed the most frequently. Results for other named
 79 *Cibicidoides* species are included, where available, but data are too sparse for a detailed
 80 analysis..

81

82 **2 Data Compilation**

83 2.1. *Cibicidoides* stable isotope data

84 This study is based on a compilation of published stable isotope data for *Cibicidoides* spp
 85 from Late Holocene (LH; 0 - ~5 kyr BP) sediment cores and core top samples (Nederbragt,
 86 2023). The $\delta^{18}\text{O}$ data were used to screen all records, to ensure that they are representative for
 87 LH. Glacial foraminifera can be present at the sediment surface in areas of slow sedimentation,
 88 causing $\delta^{18}\text{O}$ to be higher than the expected modern value (Matsumoto & Lynch-Stieglitz, 1999).
 89 Stratigraphic data were therefore checked for the presence of the expected Holocene plateau in
 90 $\delta^{18}\text{O}$ and/or ≥ 1.5 ‰ offset with Last Glacial Maximum (LGM) values (Duplessy et al., 2002;
 91 Lisiecki & Raymo, 2005). For undated core top samples, the measured $\delta^{18}\text{O}$ was compared to the
 92 expected value based on the temperature at the sea floor, and outliers were excluded (Fig. 1). The
 93 expected $\delta^{18}\text{O}$ value is calculated from an experimental temperature equation for inorganic
 94 calcite (Kim & O'Neil, 1997) adjusted to the conventionally used CO_2 -calcite fractionation
 95 factor (Bohm et al., 2000).

96 The taxonomic classification of the species included in this study has been discussed
 97 elsewhere (Holbourn et al., 2013; Schweizer, 2006). Here, all species are assigned to the genus
 98 *Cibicidoides*. Species names are copied as published without adjustment for synonymy. As
 99 shown in section 3.1, the $\delta^{13}\text{C}$ of *C. wuellerstorfi* is higher than that of other *Cibicidoides* species
 100 in the same sample. A large amount of published data has been measured on mixed *Cibicidoides*
 101 species without further specification. Such data are not included because changes in the
 102 proportion of *C. wuellerstorfi* relative to other species may distort any correlation with ambient
 103 sea water chemistry. The abbreviation "Cspp" is here used when discussing single-species results
 104 for *Cibicidoides* species other than *C. wuellerstorfi*; the informal term "mixed Cib" is reserved
 105 for unnamed mixed species.

106 2.2. Oceanographic data

107 Oceanographic data were compiled from $1^\circ \times 1^\circ$ gridded data sets. Temperature and
 108 salinity are taken from the 2013 version of the World Ocean Atlas (WOA13) (Boyer et al., 2013)
 109 and DIC and TA from the 2016 version of the Global Ocean Data Analysis Project (Key et al.,
 110 2004). Ocean water $\delta^{18}\text{O}$ data have been compiled by Schmidt (1999), while a reconstruction of
 111 pre-industrial $\delta^{13}\text{C}_{\text{DIC}}$ ($\delta^{13}\text{C}_{\text{DIC-PI}}$) is presented by Eide et al. (2017). The complete set of
 112 oceanographic data is limited to the open ocean South of $\sim 62^\circ\text{N}$, because invasion of
 113 anthropogenic CO_2 precludes reconstruction of $\delta^{13}\text{C}_{\text{DIC-PI}}$ in the Northern high latitudes (Eide et
 114 al., 2017). Marginal seas and silled basins are excluded as well due to sparse oceanographic data
 115 availability. For each core locality, oceanographic data were copied from the nearest depth level
 116 at the grid-point for the locality. If not available, values were extracted preferably as the mean
 117 for surrounding grid points, otherwise the next shallower depth-level was used. In a few cases
 118 values are taken from more distant grid points.

119 For illustration purposes, core localities are sub-divided into five ocean regions based on
 120 oceanographic characteristics (Fig. 2). The northern boundary of the Antarctic Circumpolar
 121 Current at 38°S is used to delineate the Southern Ocean (Talley et al., 2011). Atlantic localities N
 122 of 38°S (nAtl) represent low [DIC] and relatively high T, while Indo-Pacific sites N of 38°S
 123 (nIPac) have high [DIC] and low T. Most of the deep water localities (>1.5 km) South of 38°S
 124 are within the Circumpolar Deep Water (CDW) and, below 4 km, the Antarctic Bottom Water
 125 (Emery, 2001). They are split into an Atlantic sector (sAtl) and Indo-Pacific region (sIPac), both
 126 of which have intermediate [DIC]. However, the two regions differ in water temperature. Most
 127 sAtl sites show very low temperatures ($0\text{-}1^\circ\text{C}$) due to mixing of the extremely cold Weddell Sea
 128 Bottom Water into CDW (Gill, 1973; Talley et al., 2011). In contrast, values in the sIPac are
 129 higher ($1\text{-}3^\circ\text{C}$) and similar to temperatures found throughout the deep Indo-Pacific. Most shallow
 130 sites (<1.5 km) in the southern Indo-Pacific (shallow sIPac) belong to Antarctic Intermediate
 131 Water (AAIW) based on their comparatively low salinities (<34.6 PSU; Emery (2001)).
 132 However, the main reason here to group them separately is because they stand out from deeper
 133 Indo-Pacific water masses in having lower [DIC] (Fig. 2).

134

135 2.3 Carbonate chemistry

136 Concentrations of dissolved carbonate species were solved iteratively from [DIC] and
 137 [TA] using a published macro (Emerson & Hedges, 2008), except that the chemical constants K1
 138 and K2 are calculated using functions presented by Millero (1995) and Millero et al. (2006). The
 139 degree of carbonate saturation for calcite is expressed either as a ratio:

$$140 \quad \Omega_{\text{cal}} = [\text{Ca}^{2+}][\text{CO}_3^{2-}]/K_{\text{cal}} \quad (\text{Eq. 1}),$$

141 in which K_{cal} is the solubility constant of calcite as a function of temperature, salinity,
 142 and pressure (Millero, 1995), or as the offset (in $\mu\text{mol/kg}$) between measured $[\text{CO}_3^{2-}]$ and
 143 saturated water:

$$144 \quad \Delta[\text{CO}_3^{2-}] = [\text{CO}_3^{2-}] - [\text{CO}_3^{2-}]_{\text{sat}} \quad (\text{Eq. 2}),$$

145 in which $[\text{CO}_3^{2-}]_{\text{sat}}$ is calculated from Eq.1 for $\Omega_{\text{cal}} = 1$.

146

147 2.4 Isotope notation

148 Isotope data are reported in the delta notation (δ), which expresses the isotope
 149 composition of a compound as the ‰ (permil) deviation from a standard material. The relevant
 150 scales for carbonate $\delta^{18}\text{O}$ and $\delta^{13}\text{C}$ are the older PDB (Pee Dee Belemnite) scale and its
 151 replacement the VPDB (Vienna PDB) scale; the two scales are identical for $\delta^{13}\text{C}$ but offset by
 152 0.05‰ for $\delta^{18}\text{O}$ (Mook, 2000). However, published $\delta^{18}\text{O}$ values for *Cibicidoides* species are used
 153 as reported without correction, as it is not always stated clearly in the original publication which
 154 scale is used. Offsets between measured isotope data and the expected δ values are denoted by a
 155 capital delta (Δ), e.g., $\Delta^{13}\text{C}_{\text{Cwue}} = \delta^{13}\text{C}_{\text{Cwue}} - \delta^{13}\text{C}_{\text{DIC-PI}}$. The epsilon notation (ϵ , in ‰) is used here
 156 when discussing equilibrium fractionation between two compounds (Mook, 2000) with prefixes
 157 13 and 18 to distinguish between ^{13}C and ^{18}O fractionation factors.

158

159 **3 Results**160 3.1 Correlation $\delta^{13}\text{C}$ and $\delta^{18}\text{O}$

161 Measured $\delta^{13}\text{C}$ and $\delta^{18}\text{O}$ for *C. wuellerstorfi* and *Cibicidoides* spp are plotted in Figure 1
 162 against $\delta^{13}\text{C}_{\text{DIC-PI}}$ and sea water temperature respectively. Most within-core $\delta^{18}\text{O}$ values are
 163 within a range of ± 0.6 ‰ around the value expected based on ambient temperature. However,
 164 core-top data include a high proportion of values that are substantially higher than expected (Fig.
 165 1C). A histogram of $\Delta^{18}\text{O}_{\text{Cwue}}$ values shows that most values are distributed more or less
 166 symmetrically around 0‰ but that there is a long tail of positive values (Fig. 1D). The very high
 167 $\Delta^{18}\text{O}$ values are interpreted as the result of mixing with glacial specimens in areas with low
 168 sedimentation rates. A cut-off level was determined visually based on the shape of histogram of
 169 within-core $\Delta^{18}\text{O}$, as obvious signs of reworking would have been flagged during pre-screening
 170 of the stratigraphic $\delta^{18}\text{O}$ time series. Core-top data with $\Delta^{18}\text{O} > 0.6$ ‰ were excluded as most
 171 likely affected by inclusion of glacial material. In addition, four data points with $\Delta^{18}\text{O} < -0.8$ ‰
 172 were excluded as too low, possibly related to down-slope transport. The final $\Delta^{18}\text{O}$ data indicate
 173 that *C. wuellerstorfi* and *Cibicidoides* spp have the same $\Delta^{18}\text{O}$ signature (Fig. 1C, D), with mean
 174 and standard deviation of -0.03 ± 0.24 ‰ ($n = 252$), and -0.01 ± 0.23 (n = 29) respectively.

175 In contrast to $\Delta^{18}\text{O}$, the results for $\Delta^{13}\text{C}$ are not very sensitive to inclusion of reworked or
 176 bioturbated material (Fig. 1A, B). The majority of $\delta^{13}\text{C}_{\text{Cwue}}$ data (168 out of 252 data points) are
 177 slightly higher than ambient $\delta^{13}\text{C}_{\text{DIC-PI}}$. However, lower than ambient values are common for
 178 locations in sAtl and deep nAtl. Data that were excluded based on their $\Delta^{18}\text{O}$ do not stand out
 179 from other $\delta^{13}\text{C}$ data, neither in the cross plot against $\delta^{13}\text{C}_{\text{DIC-PI}}$ (Fig. 1A), nor in the histogram of
 180 $\Delta^{13}\text{C}$ (Fig. 1B). The mean and standard deviation for all $\Delta^{13}\text{C}_{\text{Cwue}}$ data is 0.04 ± 0.27 ‰.
 181 Compared to *C. wuellerstorfi*, other *Cibicidoides* spp are slightly lower, with $\Delta^{13}\text{C}_{\text{Cwue}} = -0.24 \pm$
 182 0.31 ‰ (Fig 1A, B) but the difference is not statistically significant.

183 A cross-plot of $\Delta^{13}\text{C}$ and $\Delta^{18}\text{O}$ for all *Cibicidoides* data included here shows that the two
 184 isotope offsets are significantly correlated (Fig. 3A). The correlation coefficients for *C.*
 185 *wuellerstorfi* and *Cibicidoides* spp are respectively $r = 0.30$ ($n = 252$, $P_{(r=0)} < 10^{-5}$) and $r = 0.69$ (n
 186 $= 29$, $P_{(r=0)} < 10^{-4}$). The orthogonal regression lines for *C. wuellerstorfi* and *Cibicidoides* spp are
 187 nearly parallel but offset by ~ 0.3 ‰ in $\Delta^{13}\text{C}$ for the same $\Delta^{18}\text{O}$. Paired analyses of *C.*
 188 *wuellerstorfi* and *Cibicidoides* spp are available for 13 locations (Fig. 3B, C). Visual inspection
 189 of the cross plots indicates that *C. wuellerstorfi* has higher $\Delta^{13}\text{C}$ than other *Cibicidoides* spp but

190 that $\Delta^{18}\text{O}$ values are similar. The difference in $\Delta^{13}\text{C}$ between paired *C. wuellerstorfi* and
 191 *Cibicidoides* spp ($0.21 \pm 0.26\text{‰}$) is not statistically significant but it is similar to the offset in the
 192 data set as a whole (Figs. 1, 3A).

193 A further feature to note is that between-sample variability in $\delta^{13}\text{C}_{\text{Cwu}}$ is high in areas
 194 where $\Delta^{13}\text{C}_{\text{Cwue}}$ is negative. The standard deviation for multiple analyses of *C. wuellerstorfi* in
 195 the same core is shown in Figure 3 D and E. There is a strong negative correlation between
 196 $\Delta^{13}\text{C}_{\text{Cwue}}$ and the between-sample standard deviation ($r = -0.60$, $P_{(r=0)} \ll 10^{-5}$). That is, in areas
 197 where $\Delta^{13}\text{C}_{\text{Cwue}} < 0$ the reproducibility of repeated $\delta^{13}\text{C}$ analyses is poor. In contrast, the
 198 variability of $\Delta^{18}\text{O}_{\text{Cwue}}$ is independent of the measured value ($r = -0.04$).

199

200 3.2 stable isotope composition and carbonate chemistry

201 3.2.1 bivariate correlation patterns

202 Correlation coefficients for $\Delta^{13}\text{C}_{\text{Cwue}}$ and $\Delta^{18}\text{O}_{\text{Cwue}}$ with the oceanographic variables used
 203 in this study are shown in Table 1, as well as selected coefficients for oceanographic variables
 204 amongst each other. The bivariate correlation between $\Delta^{13}\text{C}_{\text{Cwue}}$ and all oceanographic variables
 205 is significant at the 99% confidence level. For $\Delta^{18}\text{O}_{\text{Cwue}}$ the correlation is less pronounced.
 206 Notably, the correlation between $\Delta^{18}\text{O}$ and sea water temperature is not significant. Results here
 207 confirm the conclusion of Schmittner et al. (2017), that $\Delta^{13}\text{C}_{\text{Cwue}}$ correlates with water depth. Both
 208 $\Delta^{13}\text{C}$ and $\Delta^{18}\text{O}$ correlate significantly with water depth with $r = -0.468$ and $r = -0.381$
 209 respectively; in both cases $P_{(r=0)} \ll 10^{-5}$. Indeed, the correlation with depth is amongst the
 210 strongest in the data set as a whole and is exceeded only by the correlation with $[\text{CO}_2]_{\text{aq}}$ or $f\text{CO}_2$
 211 (Table 1).

212 However, the correlation between the isotope offsets and water depth is not a simple
 213 global relation. Cross plots of $\Delta^{13}\text{C}_{\text{Cwue}}$ against selected variables show that the relation depends
 214 on geographic location (Fig. 4). Results for $\Delta^{18}\text{O}_{\text{Cwue}}$ are broadly similar although the correlation
 215 is less pronounced (Figure S1). Amongst the oceanographic variables, water depth, temperature
 216 and carbonate saturation (Ω_{cal} and $\Delta[\text{CO}_3^{2-}]$) correlate strongly with each other, but less so with
 217 other variables (Table 1). These variables are here loosely grouped as "depth-related variables".
 218 They correlate with $\Delta^{13}\text{C}_{\text{Cwue}}$ especially when data are split according to ocean region (Fig. 4a-c).
 219 Values for the nAtl and nPac are offset from each other by $\sim 0.3\text{‰}$ on average. However, the
 220 magnitude of change with water depth ($0.1\text{‰}/\text{km}$), temperature ($0.1\text{‰}/^\circ\text{C}$) and $\Delta[\text{CO}_3^{2-}]$ (0.1‰
 221 per 16-20 $\mu\text{mol}/\text{kg}$) is the same in both ocean regions (Fig. 4a-c). Results for southern locations
 222 are less well defined.

223 In contrast to the depth related variables, the concentration of dissolved carbonate species
 224 varies between ocean basins (Broecker & Peng, 1982; Key et al., 2004), with high [DIC], [TA],
 225 and $[\text{HCO}_3^-]$ and low pH and $[\text{CO}_3^{2-}]$ in the nPac compared to the nAtl with little or no overlap
 226 between the two regions; intermediate values are confined to the sAtl and sPac (Fig. 2, 4d, e).
 227 All these variables are all strongly correlated with each other with $|r| \geq 0.9$ as well as with
 228 $\Delta^{13}\text{C}_{\text{Cwue}}$ (Table 1). As a result, there is a positive correlation in the full suite of data between
 229 $\Delta^{13}\text{C}_{\text{Cwue}}$ and [DIC], due to and overall trend from low $\Delta^{13}\text{C}_{\text{Cwue}}$ /low [DIC] in the Atlantic to high
 230 $\Delta^{13}\text{C}_{\text{Cwue}}$ /high [DIC] in the Indo-Pacific (Fig. 4d). A similar pattern is found for pH (Fig. 4e) and
 231 TA, $[\text{HCO}_3^-]$, and $[\text{CO}_3^{2-}]$ (not shown). However, within each region separately any correlation
 232 between $\Delta^{13}\text{C}_{\text{Cwue}}$ and these carbonate chemistry variables is not significant (Table 1; Fig. 4).

233 Of the remaining variables, salinity, $[\text{CO}_2]_{\text{aq}}$, and $f\text{CO}_2$ show a pattern that is
 234 intermediate between the depth-related and carbonate-chemistry variables, in that correlations
 235 within the individual ocean regions are mostly weaker than for the data set as a whole but still
 236 significant at least in the nAtl. The cross-plot of $\Delta^{13}\text{C}_{\text{Cwue}}$ with $f\text{CO}_2$ is shown in Figure 4f as an
 237 illustration. The data for $\Delta^{18}\text{O}_{\text{Cwue}}$ follow the same trends as in $\Delta^{13}\text{C}_{\text{Cwue}}$, with the exception that
 238 none of the correlation coefficients for $\Delta^{18}\text{O}$ with oceanographic variables within nIPac are
 239 significant (Table 1; Figure S1).

240 3.2.2 multiple linear regression

241 The presence of an offset between Atlantic and Indo-Pacific data in combination with a
 242 depth-related trend in both oceans implies that at least two variables are needed to describe
 243 variation in $\Delta^{13}\text{C}_{\text{Cwue}}$ in the global data. Multiple linear regression was therefore performed with
 244 all possible pairs of oceanographic variables as the independent variables, to find which variables
 245 are the best suited to describe variation in $\Delta^{13}\text{C}_{\text{Cwue}}$ and $\Delta^{18}\text{O}_{\text{Cwue}}$ as the dependent variable. A
 246 limited number of combinations with more variables was explored also. The amount of variation
 247 explained (R^2) by the various regressions with two independent variables is listed in Table S1.
 248 Results are broadly similar for $\Delta^{13}\text{C}_{\text{Cwue}}$ and $\Delta^{18}\text{O}_{\text{Cwue}}$, however, in all cases $\Delta^{13}\text{C}$ correlates more
 249 strongly with ambient conditions than $\Delta^{18}\text{O}_{\text{Cwue}}$. For $\Delta^{13}\text{C}_{\text{Cwue}}$, the highest R^2 values are found
 250 when the isotope offsets are compared to one of the depth-related variables (depth, temperature,
 251 carbonate saturation) in combination with one of the carbonate chemistry variables. Various
 252 combinations of two independent variabilities explain more than 35% of the total variance in
 253 $\Delta^{13}\text{C}_{\text{Cwue}}$ ($R^2 \geq 0.35$), up to a maximum of 42.6% for $\Delta^{13}\text{C}_{\text{Cwue}}$ against temperature and [DIC].
 254 Since different combinations yield broadly similar results, a subjective choice is made here to
 255 select [DIC], temperature, and $\Delta[\text{CO}_3^{2-}]$ for further analysis.

256 The regression equation for $\Delta^{13}\text{C}_{\text{Cwue}}$ against [DIC] and temperature is:

$$257 \Delta^{13}\text{C}_{\text{Cwue}} = -6.212 + 0.1217T + 0.0026[\text{DIC}] \text{ (eq. 3),}$$

258 which explains 42.6% of the total variance. The amount of variance explained is slightly
 259 lower (39.1%) for the regression for $\Delta^{13}\text{C}_{\text{Cwue}}$ against $\Delta[\text{CO}_3^{2-}]$ and [DIC]:

$$260 \Delta^{13}\text{C}_{\text{Cwue}} = -7.283 + 0.0080\Delta[\text{CO}_3^{2-}] + 0.0032[\text{DIC}] \text{ (eq. 4).}$$

261 Equations 3 and 4 are shown as contour plots in Figure 5. The amount of variance
 262 explained can be increased further to 47.1% if both temperature and $\Delta[\text{CO}_3^{2-}]$ are used in
 263 combination with [DIC]:

$$264 \Delta^{13}\text{C}_{\text{Cwue}} = -7.424 + 0.0042\Delta[\text{CO}_3^{2-}] + 0.0032[\text{DIC}] + 0.0815T, \text{ (eq. 5).}$$

265 The Standard Error on the estimate (SE) is 0.21 for Eq. 3 and 4 and SE = 0.20 for Eq. 5;
 266 the errors on the regression constants vary between 8 - 22%. The maximum amount of explained
 267 variance in $\Delta^{13}\text{C}_{\text{Cwue}}$ is 50.3% when all 12 oceanographic variables are included in the regression
 268 analysis simultaneously.

269

270 For $\Delta^{18}\text{O}_{\text{Cwue}}$, the amount of variance explained by ambient conditions is noticeably
 271 lower than for $\Delta^{13}\text{C}_{\text{Cwue}}$ (Table S1). The maximum explained variance is 35.3% when all
 272 variables are used in the regression analysis. Regression of $\Delta^{18}\text{O}_{\text{Cwue}}$ against [DIC] and $\Delta[\text{CO}_3^{2-}]$
 273 and against [DIC] and temperature accounts for respectively 19.4% and 18.7% of the total

274 variation. The equation for $\Delta^{18}\text{O}_{\text{Cwue}}$ against [DIC] and $\Delta[\text{CO}_3^{2-}]$ is shown for illustration
 275 purposes to allow comparison with the results for $\Delta^{13}\text{C}_{\text{Cwue}}$:

$$276 \quad \Delta^{18}\text{O}_{\text{Cwue}} = -4.829 + 0.0046\Delta[\text{CO}_3^{2-}] + 0.0021[\text{DIC}] \text{ (eq. 6),}$$

277 which explains 19.4% of the variation, with SE = 0.22.

278 Equations 3-6 are applied to LGM reconstructions to illustrate the magnitude of change
 279 in $\Delta^{13}\text{C}_{\text{Cwue}}$ and $\Delta^{18}\text{O}_{\text{Cwue}}$ that can be expected in response to climate change (Table 2).

280 3.2.3 Other *Cibicidoides* spp.

281 Data for named *Cibicidoides* species other than *C. wuellerstorfi* are limited to a few areas
 282 in the Atlantic and shallow sIPAC, which have low to intermediate [DIC] (Fig. 6, Nederbragt
 283 (2023)). Data from areas with high [DIC] in the Pacific are lacking. As a result, the data cover
 284 only a subset of the full range of oceanographic conditions (Fig. 6). Similar to $\Delta^{13}\text{C}_{\text{Cwue}}$, $\Delta^{13}\text{C}_{\text{Csp}}$
 285 correlates positively with $\Delta[\text{CO}_3^{2-}]$ ($r = 0.58$; $P_{(r=0)} = 4 \cdot 10^{-4}$) but in contrast the correlation with
 286 [DIC] is negative ($r = -0.48$; $P_{(r=0)} = 0.004$). The latter can be attributed to the selection of core
 287 localities: paired $\Delta^{13}\text{C}_{\text{Cwue}}$, which are available for a subset of the data, also show a negative
 288 correlation with [DIC] ($r = -0.73$; $n = 16$; $P_{(r=0)} = 0.007$) in contrast to the positive correlation
 289 within the data set as a whole (Table 1).

290

291 4 Discussion

292 4.1 Water mass characteristics and *C. wuellerstorfi* isotope composition

293 Amongst deep water benthic foraminifera the genus *Cibicidoides* has been considered as
 294 an accurate recorder of ambient $\delta^{13}\text{C}_{\text{DIC}}$ (Curry et al., 1988; Duplessy et al., 1984; McCorkle et
 295 al., 1990; Schmittner et al., 2017; Zahn et al., 1986). Based on analysis of *C. wuellerstorfi*
 296 mainly, but including some data from mixed species, Duplessy et al. (1984) concluded that $\delta^{13}\text{C}$
 297 of *Cibicidoides* spp remained in a narrow range around the expected value in a set of 44 globally
 298 distributed localities; the authors reported a mean $\Delta^{13}\text{C}_{\text{Cib}}$ and standard deviation of $0.07 \pm$
 299 0.15‰ . Since then the number of studied sections has increased. The mean value for $\Delta^{13}\text{C}_{\text{Cwue}}$ in
 300 the current compilation of 252 locations remains essentially unchanged; however, the recorded
 301 variability is nearly twice as high ($\Delta^{13}\text{C}_{\text{Cwue}} = 0.04\text{‰} \pm 0.27\text{‰}$, section 3.1). The relatively low
 302 variability found in early studies appears largely due to the almost complete absence of material
 303 from water depths below 4 km and the southern latitudes in the Atlantic Ocean (Duplessy et al.,
 304 1984). Subsequent sampling of the deep Atlantic and especially the Atlantic sector of the
 305 Southern Ocean revealed that $\Delta^{13}\text{C}_{\text{Cib}}$ can be substantially lower than expected (Hodell et al.,
 306 2003; Mackensen et al., 1993).

307 Mackensen et al. (1993) first reported the systematic occurrence of negative $\Delta^{13}\text{C}_{\text{Cib}}$
 308 along a transect South of 35°S in the South Atlantic. The authors suggested that $\delta^{13}\text{C}$ of
 309 *Cibicidoides* spp was influenced by isotopically light CO_2 from re-mineralisation of organic
 310 matter within a seasonal phytodetritus layer. It is indeed well established that infaunal benthic
 311 foraminifera can have very low $\delta^{13}\text{C}$ due to organic matter decomposition within the sediment
 312 (McCorkle et al., 1990). Phytodetritus deposits are an important food source for benthic
 313 foraminifera in the deep sea, and may well affect epifaunal benthic organisms. However,
 314 phytodetritus deposits are not limited to specific regions or water depths, but can occur anywhere

315 (Gooday, 2002; Moodley et al., 2005). In contrast, strongly negative $\Delta^{13}\text{C}_{\text{Cwue}}$ values ($<-0.40\%$)
 316 are common in the sAtl below 2.5 km and the deep Atlantic below 3.5 km, but they occur rarely
 317 elsewhere (Fig. 4A) (Schmittner et al., 2017). It is therefore likely that the presence of very low
 318 $\Delta^{13}\text{C}_{\text{Cwue}}$ is linked to a feature that is unique to the southern South Atlantic. In addition, $\Delta^{18}\text{O}_{\text{Cwue}}$
 319 is affected in tandem with $\Delta^{13}\text{C}_{\text{Cwue}}$ (Fig. 3). This suggests that there are similarities with other
 320 groups of calcifying organisms that show a link between carbonate chemistry and stable isotope
 321 composition (Krief et al., 2010; Juranek et al., 2003; McConnaughey, 1989a; Spero et al., 1997;
 322 Ziveri et al., 2012). Results found here indicate that the very low temperatures, due to mixing
 323 with WSBW, and strong undersaturation are important factors that contribute to strongly
 324 negative $\Delta^{13}\text{C}_{\text{Cwue}}$ values in the deep southern South Atlantic. In the following sections the
 325 relative importance of chemical equilibrium reactions versus biological, or vital, effects is
 326 discussed. The fact that a large number of locations are situated in the lysocline ($\Delta[\text{CO}_3^{2-}]<0$;
 327 Fig. 4) suggests that post mortem dissolution may play a role as well. However, there is
 328 insufficient published information on the preservation of *Cibicidoides spp* to evaluate its
 329 importance.

330

331 4.2 Multiple linear regression

332 Multiple linear regression is used here to illustrate the relation between $\Delta^{13}\text{C}_{\text{Cwue}}$ and
 333 ambient conditions. However, the predictive potential of all regression equations (Eq 3-6) is low.
 334 With the relatively low amount of variance explained by Eqs 3-6 ($<50\%$) any confidence
 335 intervals around a new observation would be wider than the spread in the entire isotope data set
 336 (Sokal & Rohlf, 1994). Furthermore, the presence of collinearity, i.e., the strong correlation
 337 between the oceanographic variables used in this study (Table 1), complicates the interpretation
 338 of regression coefficients. The explained variance is partitioned more or less arbitrarily between
 339 the independent variables when they are intercorrelated (Farrar & Glauber, 1967; Nimon &
 340 Oswald, 2013). Although there are various methods to improve the regression model (Nimon &
 341 Oswald, 2013), interpretation of the relative importance of the various variables remains
 342 somewhat subjective.

343 The offset between $\Delta^{13}\text{C}_{\text{Cwue}}$ in the Atlantic and Indo-Pacific Oceans is here described
 344 using [DIC] in combination with temperature and/or $\Delta[\text{CO}_3^{2-}]$ (Fig. 5). Several studies have
 345 found that the isotope composition of biogenic carbonate is dependent on ambient carbonate
 346 chemistry. The effect is described variously as a response to changing pH or $[\text{CO}_3^{2-}]$ (Spero et
 347 al., 1997; Zeebe, 1999; Ziveri et al., 2012). However, in practice pH, $[\text{CO}_3^{2-}]$, [DIC] and [TA]
 348 are highly correlated in the world oceans (Table 1) such that it is difficult to decide if any
 349 specific variable is the underlying cause of the change in isotope composition. The choice here to
 350 use [DIC] rather than pH is based on the fact that it is conceptually linked with $\delta^{13}\text{C}_{\text{Cwue}}$, as aging
 351 of bottom waters increases [DIC] but decreases $\delta^{13}\text{C}_{\text{DIC}}$ through the remineralisation of sinking
 352 organic matter in the deep ocean (Broecker & Peng, 1982; Curry et al., 1988; Duplessy et al.,
 353 1984). In addition, [DIC] and [TA] are measured directly in the modern ocean (Key et al., 2004),
 354 from which all other carbonate chemistry variables (pH, $[\text{HCO}_3^-]$, $[\text{CO}_3^{2-}]$) are calculated.

355 The depth-related variables (saturation state, temperature, and water depth or pressure)
 356 are also intercorrelated, because saturation state is strongly dependent on ambient temperature
 357 and pressure (eq 1, (Millero, 1995)). The correlation between $\Delta^{13}\text{C}_{\text{Cwue}}$ and water depth, which
 358 was previously described by (Schmittner et al., 2017), is here assumed to be indirect, because of

359 the impact of pressure on saturation state. In contrast, both saturation state and temperature are
 360 likely to have a direct impact on the biology of deep sea calcareous organisms. Carbonate
 361 saturation state determines the amount of CO_3^{2-} available for calcification, while temperature
 362 affects metabolic rates in exothermic organisms (e.g. , Bemis et al., 2000; Gillooly et al., 2001;
 363 Juranek et al., 2003; Krief et al., 2010). Of the two saturation state variables, $\Delta[\text{CO}_3^{2-}]$ has the
 364 practical advantage that it can be reconstructed from fossil material (Yu & Elderfield, 2007). The
 365 regression results confirm that temperature and saturation state each have an effect on $\Delta^{13}\text{C}_{\text{Cwue}}$.
 366 Regression equation 5, which relates $\Delta^{13}\text{C}_{\text{Cwue}}$ to both temperature and $\Delta[\text{CO}_3^{2-}]$ with [DIC],
 367 explains noticeably more variation (47.1%) than equations 3 and 4 for temperature and $\Delta[\text{CO}_3^{2-}]$
 368 separately (42.6% and 39.1% respectively). However, the actual values of the regression
 369 coefficients, which describe the magnitude of change in $\Delta^{13}\text{C}_{\text{Cwue}}$, may not reflect the real
 370 contribution of temperature relative to $\Delta[\text{CO}_3^{2-}]$ due to the collinearity between the two variables
 371 (Farrar & Glauber, 1967; Nimon & Oswald, 2013).

372

373 4.3 Stable isotope composition and ambient conditions

374 4.3.1 Temperature

375 If taken at face values, the regression coefficients for temperature in Eq. 3 (0.1217) and
 376 Eq. 5 (0.0815) imply that $\delta^{13}\text{C}$ in *C. wuellerstorfi* is highly sensitive to ambient temperature, with
 377 a shift of $\sim 0.1\text{‰}$ in $\Delta^{13}\text{C}_{\text{Cwue}}$ per 1°C . Although the $\delta^{13}\text{C}$ of various planktonic and benthic
 378 foraminiferal species is known to be affected by ambient conditions and physiological processes,
 379 the actual role of temperature is poorly constrained. Based on reinterpretation of published
 380 precipitation experiments, Mook (2000) estimated that the $\delta^{13}\text{C}$ fractionation between solid
 381 carbonate and dissolved HCO_3^- ($^{13}\epsilon_{\text{CaCO}_3/\text{HCO}_3^-}$) varies with temperature by $\sim 0.05\text{‰}/^\circ\text{C}$. This
 382 temperature equation was used to model $\delta^{13}\text{C}_{\text{Cwue}}$ in response to equilibrium diffusion of DIC
 383 around the foraminiferal shell (Hesse et al., 2014). The outcome was that the temperature
 384 sensitivity of inorganic carbonate is incorporated into the foraminiferal shell. However, it has to
 385 be noted that calcification processes within the foraminiferal cell are not included in the model
 386 (Hesse et al., 2014). In contrast to Mook (2000), Romanek et al. (1992) concluded based on
 387 another set of carbonate precipitation experiments that $^{13}\epsilon_{\text{CaCO}_3/\text{HCO}_3^-}$ remains constant between
 388 $10 - 40^\circ\text{C}$. Indeed, Bemis et al., (2000) found that $\delta^{13}\text{C}$ of *Orbulina universa* was not sensitive to
 389 changing temperature as long as it was grown under dark conditions to inhibit activity of its
 390 symbionts. However, the $\delta^{13}\text{C}$ of *O. universa* did change with temperature when grown under
 391 light conditions, due to the symbionts contributing isotopically light CO_2 . *Globerina bulloides*
 392 also showed a correlation between $\delta^{13}\text{C}$ and temperature, which was attributed to increased
 393 growth rates and enhanced incorporation of metabolic CO_2 at higher temperatures (Bemis et al.,
 394 2000). This would suggest that any correlation between foraminiferal $\delta^{13}\text{C}$ and temperature is
 395 related to vital effects rather than chemical equilibrium.

396 In contrast to $\delta^{13}\text{C}$, the temperature sensitivity of carbonate $\delta^{18}\text{O}$ due to chemical
 397 equilibrium with ambient H_2O is well established. Numerous experimental and empirical
 398 temperature equations have been published, which are offset from each other but show similar
 399 temperature dependencies with values of $-0.2 - -0.3\text{‰}/^\circ\text{C}$ depending on the actual temperature
 400 ((Bemis et al., 1998) and references there-in). Here, the $\delta^{18}\text{O}_{\text{Cwue}}$ data have been corrected for the
 401 effect of temperature using an equation established for inorganic calcite precipitation (Bohm et

402 al., 2000; Kim & O'Neil, 1997). This was an a priori choice, because all variables except
 403 temperature can be held constant under experimental conditions. However, it has to be noted that
 404 the results may not represent "true" equilibrium precipitation of carbonate, as the specific $\delta^{18}\text{O}$
 405 values are dependent on the composition of the reactants and their concentration (Kim & O'Neil,
 406 1997; Watkins et al., 2014; Zeebe, 1999). In contrast, Marchitto et al. (2014) established an
 407 empirical equation specifically for *Cibicidoides* spp, which is based mainly on data from the
 408 North Atlantic. This equation is therefore potentially biased by regional oceanic conditions. In
 409 practice, however, the offset between the two equations is $<0.2\text{‰}$ throughout the observed
 410 temperature range (Fig. 1).

411 Within the data set as a whole, the resultant $\Delta^{18}\text{O}_{\text{Cwue}}$ values are not significantly
 412 correlated with temperature (Table 1). However, any relation between $\Delta^{18}\text{O}_{\text{Cwue}}$ and temperature
 413 is potentially complicated. The equilibrium effect of temperature on $^{18}\text{E}_{\text{CaCO}_3/\text{H}_2\text{O}}$ causes a
 414 decrease in carbonate $\delta^{18}\text{O}$ as temperature increases (Kim & O'Neil, 1997). In contrast, $\Delta^{13}\text{C}_{\text{Cwue}}$
 415 increases as temperature increases (Fig. 4). Given the positive correlation between $\Delta^{18}\text{O}_{\text{Cwue}}$ and
 416 $\Delta^{13}\text{C}_{\text{Cwue}}$ (Fig. 3) and assuming that the influence of temperature on $\Delta^{13}\text{C}_{\text{Cwue}}$ is due to vital
 417 effects, the relation between $\Delta^{18}\text{O}_{\text{Cwue}}$ and temperature is expected to be the inverse of the
 418 equilibrium relation between $\delta^{18}\text{O}$ and temperature. Indeed, there is a positive correlation
 419 between $\Delta^{18}\text{O}_{\text{Cwue}}$ and temperature within the subset of Atlantic data (Table 1, Fig. S1). The lack
 420 of clear correlation in the full suite of data may therefore reflect the presence of noise due to
 421 competing equilibrium reactions and vital effects, but for practical purposes $\Delta^{18}\text{O}_{\text{Cwue}}$ is
 422 essentially independent of temperature.

423

424 4.3.2 Carbonate chemistry

425 Several culture experiments have shown that the $\delta^{18}\text{O}$ of calcareous organisms is
 426 sensitive to a change in the pH, or $[\text{CO}_3^{2-}]$, of ambient water (Krief et al., 2010; Spero et al.,
 427 1997; Ziveri et al., 2012). Although the exact mechanism is not fully understood, the large
 428 isotope contrast between CO_3^{2-} and HCO_3^- is thought to play a role. Values for $^{18}\text{E}_{\text{CO}_3^{2-}/\text{HCO}_3^-}$ are
 429 $\sim -7\text{‰}$ in the range of temperatures found in the modern ocean (Beck et al., 2005). As long as
 430 calcification involves some form of quantitative precipitation of all available DIC species, the
 431 $\delta^{18}\text{O}$ of carbonate would decrease when pH increases because isotopically light $[\text{CO}_3^{2-}]$ increases
 432 (Devriendt et al., 2017; Zeebe, 1999). Indeed, in all three culture experiments it was found that
 433 $\delta^{18}\text{O}$ decreases when pH (or $[\text{CO}_3^{2-}]$) was increased. However, the magnitude of change is
 434 species specific (Krief et al., 2010; Spero et al., 1997; Ziveri et al., 2012), suggesting that
 435 biological factors, or vital effects, play a role.

436 The response of skeletal $\delta^{13}\text{C}$ to changing pH is more variable. In contrast to $\delta^{18}\text{O}$, large
 437 changes in carbonate $\delta^{13}\text{C}$ in response to ambient pH are not expected as a result of chemical
 438 equilibrium reactions. The fractionation $^{13}\text{E}_{\text{CO}_3^{2-}/\text{HCO}_3^-}$ is too small ($\sim -0.5\text{‰}$) to allow substantial
 439 fractionation due to variation in $[\text{CO}_3^{2-}]$ and $[\text{HCO}_3^-]$ (Hesse et al., 2014; Mook, 2000). Still, co-
 440 variation between $\delta^{13}\text{C}$ and $\delta^{18}\text{O}$ was observed in two of the culture experiments mentioned
 441 (Krief et al., 2010; Spero et al., 1997). Krief et al. (2010) concluded that changes in skeletal $\delta^{13}\text{C}$
 442 in corals are mainly due to variation in photosynthesis of the symbionts and uptake of metabolic
 443 CO_2 under varying pH and pCO_2 conditions. In contrast, Spero et al (1997) could exclude the
 444 effect of symbiont activity by growing *O. universa* under low light conditions. The authors
 445 observed that $\delta^{13}\text{C}$ decreased by $\sim 4\text{‰}$ with increasing $[\text{CO}_3^{2-}]$ across a range of pH values

446 between 7.7 - 8.8, in concert with a decrease in $\delta^{18}\text{O}$ of ~ 1.5 ‰. The magnitude of change in
 447 $\delta^{18}\text{O}$ is consistent with chemical equilibrium reactions but the much larger shift in $\delta^{13}\text{C}$ requires
 448 the presence of vital effects (Bijma et al., 1999; Zeebe et al., 1999).

449 Results here for *C. wuellerstorfi* provide an example that covariation between $\delta^{13}\text{C}$ and
 450 $\delta^{18}\text{O}$ in foraminifera in response to ambient DIC also occurs under natural conditions. However,
 451 the correlation between $\Delta^{13}\text{C}_{\text{Cwue}} / \Delta^{18}\text{O}_{\text{Cwue}}$ and pH or $[\text{CO}_3^{2-}]$ is not the same as that observed in
 452 *O. universa*. There is a significant but weak negative correlation between $\Delta^{13}\text{C}_{\text{Cwue}} / \Delta^{18}\text{O}_{\text{Cwue}}$ and
 453 pH (Table 1), which is similar to the correlation observed by Spero et al (1997). However, a
 454 much stronger positive correlation with both [DIC] and $\Delta[\text{CO}_3^{2-}]$ is found when multiple
 455 variables are considered (equations 4 - 6). The negative correlation with pH is here interpreted as
 456 an artefact of the uneven distribution of sample locations across the range of conditions in the
 457 oceans (Fig. 4e). Negative $\Delta^{13}\text{C}_{\text{Cwue}}$ data are most frequent in the deep Atlantic, which has high
 458 pH, while $\Delta^{13}\text{C}_{\text{Cwue}}$ is generally positive in the Pacific, which has low pH. However, there is no
 459 significant relation between $\Delta^{13}\text{C}_{\text{Cwue}} / \Delta^{18}\text{O}_{\text{Cwue}}$ and pH within either ocean separately (Table 1).
 460 Overall, the positive correlation with $\Delta[\text{CO}_3^{2-}]$ is taken to mean that undersaturation in the deep
 461 ocean is a major factor, with $\Delta^{13}\text{C}_{\text{Cwue}} / \Delta^{18}\text{O}_{\text{Cwue}}$ decreasing when $\Delta[\text{CO}_3^{2-}]$ decreases.

462 Given the diverse responses of different organisms it seems likely that species-specific
 463 vital effects are important. In the case of *C. wuellerstorfi* and other *Cibicidoides* species such
 464 vital effects may well be related to the degree of calcite saturation in the deep ocean, either
 465 directly or indirectly.

466 4.3.3 Habitat and calcite precipitation rates

467 Benthic foraminiferal habitat is usually discussed in terms of substrate and food supply
 468 (e.g., Gottschalk et al., 2016; Jorissen et al., 1998; Lutze & Thiel, 1989; Wollenburg et al.,
 469 2018). However, the ability to calcify in undersaturated conditions may well be a another factor.
 470 Around half of all localities included in this paper are located within the lysocline, i.e., $\Delta[\text{CO}_3^{2-}]$
 471 < 0 (Fig. 4). However, foraminifera can create saturated conditions within their cell, because they
 472 raise pH internally as part of the calcification process (Bentov et al., 2009). Still, it seems
 473 plausible that undersaturated conditions equate to some form of environmental stress, and that
 474 this has an effect on the stable isotope signature (Bijma et al., 1999). It is noticeable that the
 475 variability in $\delta^{13}\text{C}_{\text{Cwue}}$ between samples increases when $\Delta^{13}\text{C}_{\text{Cwue}} < 0$ (fig. 3d). The fact that
 476 *Cibicidoides* spp can actively seek out a favourable location (Lutze & Thiel, 1989; Wollenburg
 477 et al., 2018) suggests that within the lysocline individual specimens are more likely to inhabit a
 478 range of different micro-habitats to mitigate adverse conditions in the wider environment.

479 One of the ways in which *Cibicidoides* species could modify their isotope signature is by
 480 alternating between epi- and infaunal habitats. *Cibicidoides pachyderma* (morphotype *C.*
 481 *mundulus*) has been cultured at two different pH-levels in high-pressure cells with artificial
 482 sediment (Wollenburg et al., 2018). The authors observed that the foraminifera became infaunal
 483 at pH=7.4 while specimens at pH=8.0 actively sought an epifaunal location with active water
 484 flow. If *Cibicidoides* species exhibit similar behavior under natural conditions, then the low $\Delta^{13}\text{C}$
 485 signature in the deep Atlantic could be acquired from organic matter decay within the sediment
 486 rather than from phytodetritus on the sediment surface (Mackensen et al., 1993; Wollenburg et
 487 al., 2018). However, the pH-levels applied during the experiment far exceed the range of natural
 488 values in the deep ocean (pH 7.79-7.98; Fig. 4). Furthermore, it does not explain why very low
 489 $\Delta^{13}\text{C}_{\text{Cwue}}$ occur in the deep Atlantic but rarely in the deep Pacific (Fig. 4). Lastly, there are

490 insufficient data to determine if there is a consistent relation between the habitat of *Cibicidoides*
 491 species and ambient chemistry under natural conditions. The presence/absence of suitable
 492 substrates may also play a role. Where hard substrates are available, *C. wuellerstorfi* is
 493 preferentially attached to any solid surface that is elevated above the sea floor (Lutze & Thiel,
 494 1989). In contrast, it has a shallow infaunal habitat in clayey sediments all along a depth transect
 495 off Cape Blanc, NW Africa, down to 3010 m water depth (Jorissen et al., 1998). The $\delta^{13}\text{C}_{\text{Cwue}}$
 496 was not measured in this study. However, data included here from the wider region show that
 497 conditions are generally saturated ($\Delta[\text{CO}_3^{2-}] > 0$) with $\Delta^{13}\text{C}_{\text{Cwue}} \geq -0.06\text{‰}$ in the relevant depth
 498 range (Nederbragt, 2023). For the sediments off Cape Blanc this implies that *C. wuellerstorfi* can
 499 be infaunal under saturated conditions without displaying a decrease in $\delta^{13}\text{C}$.

500 As an alternative explanation for the correlation between isotope composition of
 501 *Cibicidoides* spp and ambient carbonate chemistry I suggest that variation in saturation state has
 502 a direct effect on calcification processes within the foraminiferal test. Reduced calcification rates
 503 have been observed in response to lowering of ambient pH in various species of foraminifera
 504 (Erez (2003) and references therein; Bijma et al., 1999). A correlation between isotope
 505 composition and calcification rates has been observed in corals, although not directly in
 506 foraminifera (Bijma et al., 1999; McConnaughey, 1989a). From inorganic carbonate
 507 precipitation experiments it is known that at least $\delta^{18}\text{O}$ is dependent on the concentration of the
 508 reactants (Kim & O'Neil, 1997; Watkins et al., 2014; Zeebe, 1999). As such, the observed
 509 variation in $\Delta^{13}\text{C}$ and $\Delta^{18}\text{O}$ may well represent isotope fractionation due to vital effects within
 510 the foraminiferal test rather than variation in ambient $\delta^{13}\text{C}_{\text{DIC}}$. This does not exclude the
 511 possibility that switching between epifaunal and infaunal habitats plays a role. For example, pore
 512 water within sediment in the lysocline may have elevated levels of [DIC] or $\Delta[\text{CO}_3^{2-}]$ due to
 513 carbonate dissolution within the sediment, which would favor an infaunal habitat if ambient
 514 undersaturation is a limiting factor.

515 There may be a parallel with the inorganic calcite precipitation experiments of (Zuddas &
 516 Mucci, 1994), who studied calcite precipitation rates in high ionic strength solutions to mimic
 517 reactions in sea water. The authors found that precipitation rates increased with increasing pCO_2
 518 as well as increasing Ω_{cal} . That is, similar to the current data, two variables in the carbonate
 519 system are required to describe the observed variation. In the precipitation experiment, pCO_2
 520 was proportional to [DIC] as pCO_2 was adjusted by adding Na_2CO_3 and NaHCO_3 while
 521 maintaining constant ionic strength. Zuddas & Mucci (1994) suggested that two variables are
 522 needed to predict precipitation rates because both HCO_3^- and CO_3^{2-} contribute to the
 523 precipitation reaction. The total range of variation in pCO_2 during the experiment was three
 524 orders of magnitude larger than found under natural marine conditions. As such, results are not
 525 immediately applicable to biological carbonates formed under natural conditions. Still, it
 526 suggests that low $\Delta^{13}\text{C}_{\text{Cwue}}$ and $\Delta^{18}\text{O}_{\text{Cwue}}$ may be induced by a decrease in calcification rates in an
 527 environment with low [DIC] and $\Delta[\text{CO}_3^{2-}]$. The fact that $\Delta^{13}\text{C}_{\text{Cwue}}$ also correlates with
 528 temperature (Fig. 4B; section 4.3.1) is consistent with this hypothesis, since metabolic rates are
 529 expected to decrease when temperature decreases (Gillooly et al., 2001). In theory this
 530 hypothesis can be tested, by measuring the weight and size of single *Cibicidoides* specimens
 531 before analysing their isotope composition. However, any relation, if present, could be
 532 complicated by post-mortem dissolution because of the undersaturated environment.

533 4.3.4 Other *Cibicidoides* spp

534 Other *Cibicidoides* species are here presented as a group, because there are not enough
 535 published data for individual species to substantiate any global trends. Still, the available data
 536 suggest that the stable isotope composition of *Cibicidoides* spp correlates with ambient carbonate
 537 chemistry similar to *C. wuellerstorfi*, except that $\Delta^{13}\text{C}_{\text{Cspp}}$ is on average 0.2-0.3‰ lower than
 538 $\Delta^{13}\text{C}_{\text{Cwue}}$ (Fig. 3, 6). However, the data are highly variable while covering only a relatively
 539 narrow range of oceanographic conditions. The offset between $\Delta^{13}\text{C}_{\text{Cwue}}$ and $\Delta^{13}\text{C}_{\text{Cspp}}$ is
 540 therefore not statistically different from zero, and it is not clear if the offset is constant or
 541 depends on oceanographic conditions.

542 The suggestion that $\delta^{13}\text{C}_{\text{Cwue}} - \delta^{13}\text{C}_{\text{Cspp}}$ is dependent on ambient conditions was raised by
 543 Gottschalk et al. (2016). The authors observed that the offset between *C. wuellerstorfi* and *C.*
 544 *kullenbergi* changed from $\sim 0.25\text{‰}$ in the Holocene to $\sim 0.75\text{‰}$ during the last glacial in a set of
 545 sediment cores from the southern South Atlantic. In one of the cores (TTN057-6), the increased
 546 glacial offset in $\delta^{13}\text{C}$ coincides with lower $\Delta[\text{CO}_3^{2-}]$, as indicated by lower carbonate content and
 547 increased fragmentation of planktonic foraminifera (Hodell et al., 2003). *Cibicidoides*
 548 *kullenbergi* (or *C. mundulus* depending on the synonymy used) has a habitat ranging from
 549 bathyal to abyssal, while *C. wuellerstorfi* is primarily bathyal (Holbourn et al., 2013). This
 550 suggests that *C. mundulus/kullenbergi* can withstand more severely undersaturated conditions
 551 than *C. wuellerstorfi*. Possibly, the more extreme habitat is accompanied by a further decrease in
 552 $\Delta^{13}\text{C}_{\text{Cspp}}$.

553 However, it is not clear if there is a consistent correlation between the offset $\delta^{13}\text{C}_{\text{Cwue}} -$
 554 $\delta^{13}\text{C}_{\text{Cspp}}$ and saturation state. The glacial deep Atlantic was more undersaturated than the modern
 555 ocean (Yu et al., 2013), yet both *C. wuellerstorfi* and mixed-Cib show the same change in $\delta^{13}\text{C}$
 556 between LGM and LH values on average. The shift is $0.63 \pm 0.35 \text{‰}$ for *C. wuellerstorfi* ($n = 99$)
 557 compared to $0.65 \pm 0.35 \text{‰}$ for mixed-Cib ($n = 44$) at depths $>2.5 \text{ km}$ (data from (Hesse et al.,
 558 2011; Peterson et al., 2014)). On the other hand, mixed-Cib includes *C. wuellerstorfi* in unknown
 559 proportions and may not be representative for *C. mundulus/kullenbergi*. A further complication is
 560 that different morphotypes within a given species may have a different isotope signature
 561 (Gottschalk et al., 2016), which means that differences in species concept between authors may
 562 also play a role. Until further data become available the offset $\delta^{13}\text{C}_{\text{Cwue}} - \delta^{13}\text{C}_{\text{Cspp}}$ is best assumed
 563 to be variable ($0.21 \pm 0.26\text{‰}$, section 3.1) but not dependent on ambient conditions.

564

565 **5 Conclusions and paleoceanographic implications**

566 Variation in carbonate chemistry in the deep sea explains up to 50.3% and 35.3% of the
 567 variance in $\Delta^{13}\text{C}_{\text{Cwue}}$ and $\Delta^{18}\text{O}_{\text{Cwue}}$ respectively. Both $\Delta^{13}\text{C}_{\text{Cwue}}$ and $\Delta^{18}\text{O}_{\text{Cwue}}$ increase when
 568 $[\text{DIC}]$ and $\Delta[\text{CO}_3^{2-}]$ increase, while only $\Delta^{13}\text{C}_{\text{Cwue}}$ correlates with temperature. The underlying
 569 mechanism is discussed in terms of chemical equilibrium, kinetic effects, and vital effects, but
 570 remains essentially unknown. A link with reduced calcification in undersaturated conditions in
 571 the deep ocean is suggested. Remaining variation cannot be attributed. It may represent a
 572 combination of random noise and analytical error, as well as systematic variation due to
 573 environmental factors that are not considered here, like food supply, substrate, or post-mortem
 574 dissolution (Corliss et al., 2006; Jorissen et al., 1998; Lutze & Thiel, 1989; Wollenburg et al.,
 575 2018).

576 To illustrate the magnitude of change in $\Delta^{13}\text{C}_{\text{Cwue}}$ and $\Delta^{18}\text{O}_{\text{Cwue}}$ that can be expected
 577 when oceanic conditions change, equations 3-6 have been applied to LGM conditions (Table 2).
 578 During LGM, deep oceans everywhere were close to freezing (Adkins et al., 2002; Duplessy et
 579 al., 2002). Assuming that both the deep Pacific and Atlantic were around -1°C implies that
 580 temperatures were lower by 2.5°C and 3.5°C respectively compared to LH (Fig. 2). The oceanic
 581 carbon budget during LGM is estimated at 38,000 Gt, which is 1.5 Gt, or 2%, higher than the
 582 pre-industrial value (Sundquist, 1993). Assuming the increase in carbon to be distributed evenly
 583 across all water masses implies that [DIC] during LGM was $\sim 45\mu\text{mol/kg}$ higher than modern.
 584 Lastly, during LGM, $\Delta[\text{CO}_3^{2-}]$ was similar to LH values in the Pacific but the Atlantic was more
 585 undersaturated by $-20\mu\text{mol/kg}$ (Anderson & Archer, 2002; Yu et al., 2013).

586 The effect on $\Delta^{18}\text{O}_{\text{Cwue}}$ is minor compared the total variability in the $\delta^{18}\text{O}$ data. Overall,
 587 $\Delta^{18}\text{O}_{\text{Cwue}}$ is expected to change by $\leq 0.1\text{‰}$ in response to glacial/interglacial variation in [DIC]
 588 and $\Delta[\text{CO}_3^{2-}]$ (Table 2), a value that is negligible compared to the $\sim 1.5\text{‰}$ change in $\delta^{18}\text{O}_{\text{Cwue}}$ due
 589 to ice cap effects and changing deep sea temperatures (Duplessy et al., 2002; Lisiecki & Raymo,
 590 2005). However, the effect of changing $\Delta[\text{CO}_3^{2-}]$ can play a role in the evaluation of coupled
 591 Mg/Ca - $\delta^{18}\text{O}$ data. $\Delta^{18}\text{O}_{\text{Cwue}}$ is less sensitive to changes in saturation state than the Mg/Ca
 592 composition of *C. wuellerstorfi* but the two reinforce each other. That is, the effect of salinity
 593 needed to explain paired Mg/Ca - $\delta^{18}\text{O}$ data will be overestimated. A change of $-20\mu\text{mol/kg}$ in
 594 $\Delta[\text{CO}_3^{2-}]$ for LGM-LH in the deep Atlantic is expected to effect a ~ -0.17 mmol/mol change in
 595 Mg/Ca, which is equivalent to -1 to -2°C depending on actual temperature (Elderfield et al.,
 596 2006; Yu et al., 2013). The equivalent effect on $\Delta^{18}\text{O}_{\text{Cwue}}$ is $\sim -0.09\text{‰}$ (Table 2), or $+0.4$ to $+0.5$
 597 $^\circ\text{C}$.

598 By contrast, glacial/interglacial changes in $\Delta^{13}\text{C}_{\text{Cwue}}$ are potentially a substantial part of
 599 the total variation in $\delta^{13}\text{C}_{\text{Cwue}}$. During LGM $\delta^{13}\text{C}_{\text{DIC}}$ was lighter than modern, due to reduced
 600 storage of terrestrial carbon in combination with changes in water mass circulation (Duplessy et
 601 al., 1984; Peterson et al., 2014; Sundquist, 1993). The measured difference in $\delta^{13}\text{C}_{\text{Cib}}$ between
 602 LH-LGM is $\sim 0.35\text{‰}$ in the deep Pacific and $\sim 0.65\text{‰}$ in the deep Atlantic (Curry et al., 1988;
 603 Duplessy et al., 2002; Hesse et al., 2011; Hodell et al., 2003; Peterson et al., 2014). By
 604 comparison, a decrease of up to 0.2‰ and 0.3‰ in $\Delta^{13}\text{C}_{\text{Cwue}}$ may have occurred in response to
 605 changing oceanographic conditions in the deep Pacific and Atlantic respectively (Table 2), which
 606 is equivalent to up to half the observed shift in LH-LGM $\delta^{13}\text{C}_{\text{Cib}}$ in nAtl and nPac.

607 The largest offset between LH-LGM $\delta^{13}\text{C}_{\text{Cib}}$ has been found in the Southern Ocean, with
 608 LGM values up to 1.3‰ lower than modern (Hodell et al., 2003; Peterson et al., 2014). The low
 609 in $\delta^{13}\text{C}_{\text{Cib}}$ is attributed to the presence of old SCW with high [DIC] (Hodell & Venz-Curtis,
 610 2006; Sigman et al., 2010) and/or reduced air-sea exchange in Antarctic surface waters causing
 611 lower preformed $\delta^{13}\text{C}_{\text{DIC}}$ (Broecker & Maier-Reimer, 1992; Mackensen, 2012). Results here
 612 suggest a third possibility, that low $\delta^{13}\text{C}_{\text{Cwue}}$ reflects a further decrease in $\Delta^{13}\text{C}_{\text{Cwue}}$ under glacial
 613 conditions without much change in $\delta^{13}\text{C}_{\text{DIC}}$ other than the decrease that occurred globally. In the
 614 modern ocean, low $\delta^{13}\text{C}_{\text{Cwue}}$ ($\leq 0\text{‰}$ VPDB) is found both in the Pacific and the deep South
 615 Atlantic (Fig. 2). Looking at $\delta^{13}\text{C}_{\text{Cwue}}$ only, the two ocean regions are distinct in the
 616 reproducibility of repeated measurements. In the Pacific, with high [DIC], between-sample
 617 reproducibility of $\delta^{13}\text{C}_{\text{Cwue}}$ is good and $\Delta^{13}\text{C}_{\text{Cwue}} \geq 0$, while in SAtl sections, which have low to
 618 intermediate [DIC], $\delta^{13}\text{C}_{\text{Cwue}}$ is highly variable and $\Delta^{13}\text{C}_{\text{Cwue}} < 0$ (Fig. 1, 3). The wide scatter
 619 found in modern sAtl data is also apparent in glacial data from this region (Hodell et al., 2003;
 620 Ninnemann & Charles, 2002); the analogue with modern data implies that [DIC] during LGM in

621 SO was not very high, i.e., that SCW water masses were not substantially older than they are
622 currently.

623 **Acknowledgments**

624 H.J. Spero, an anonymous reviewer, and associate editor all provided helpful comments
625 to improve an earlier version of the manuscript. This is Cardiff EARTH CRediT Contribution 20.

626 **Open Research**

627 The full compilation of isotope data and oceanographic data has been archived at the
628 world data centre Pangaea (Nederbragt, 2023).

629 **References**

- 630 Adkins, J. F., McIntyre, K., & Schrag, D. P. (2002). The salinity, temperature, and $\delta^{18}\text{O}$ of the
631 glacial deep ocean. *Science*, 298(5599), 1769-1773. doi:10.1126/science.1076252
- 632 Anderson, D. M., & Archer, D. (2002). Glacial-interglacial stability of ocean pH inferred from
633 foraminifer dissolution rates. *Nature*, 416(6876), 70-73. doi:10.1038/416070a
- 634 Armstrong, R. A., Lee, C., Hedges, J. I., Honjo, S., & Wakeham, S. G. (2002). A new,
635 mechanistic model for organic carbon fluxes in the ocean based on the quantitative
636 association of POC with ballast minerals. *Deep-Sea Research Part II-Topical Studies in
637 Oceanography*, 49(1-3), 219-236. doi:10.1016/S0967-0645(01)00101-1
- 638 Beck, W. C., Grossman, E. L., & Morse, J. W. (2005). Experimental studies of oxygen isotope
639 fractionation in the carbonic acid system at 15°, 25°, and 40°C. *Geochimica et
640 Cosmochimica Acta*, 69(14), 3493-3503. doi:10.1016/j.gca.2005.02.003
- 641 Bemis, B. E., Spero, H. J., Bijma, J., & Lea, D. W. (1998). Reevaluation of the oxygen isotopic
642 composition of planktonic foraminifera: experimental results and revised
643 paleotemperature equations. *Paleoceanography*, 13(2), 150-160. doi:10.1029/98PA00070
- 644 Bemis, B. E., Spero, H. J., Lea, D. W., & Bijma, J. (2000). Temperature influence on the carbon
645 isotopic composition of *Globigerina bulloides* and *Orbulina universa* (planktonic
646 foraminifera). *Marine Micropaleontology*, 38(3-4), 213-228. doi:10.1016/s0377-
647 8398(00)00006-2
- 648 Bentov, S., Brownlee, C., & Erez, J. (2009). The role of seawater endocytosis in the
649 biomineralization process in calcareous foraminifera. *Proceedings of the National
650 Academy of Sciences of the United States of America*, 106(51), 21500-21504.
651 doi:10.1073/pnas.0906636106
- 652 Bijma, J., Spero, H. J., & Lea, D. W. (1999). Reassessing foraminiferal stable isotope
653 geochemistry: Impact of the oceanic carbonate system (experimental results). In G.
654 Fischer & G. Wefer (Ed.), *Use of Proxies in Paleoceanography: Examples from the
655 South Atlantic* (pp. 489-512). New York: Springer-Verlag.

- 656 Bohm, F., Joachimski, M. M., Dullo, W. C., Eisenhauer, A., Lehnert, H., Reitner, J., &
 657 Worheide, G. (2000). Oxygen isotope fractionation in marine aragonite of coralline
 658 sponges. *Geochimica et Cosmochimica Acta*, *64*(10), 1695-1703. doi:10.1016/S0016-
 659 7037(99)00408-1
- 660 Boyer, T. P., Antonov, J. I., Baranova, O. K., Coleman, C., Garcia, H. E., Grodsky, A., et al.
 661 (2013). World Ocean Database 2013. In S. Levitus & A. Mishonov (Eds.), *NOAA Atlas*
 662 *NESDIS 72* (pp. 209 pp (<http://doi.org/10.7289/V5NZ85MT>)). Silver Spring, MD, USA.
- 663 Broecker, W. S., & Maier-Reimer, E. (1992). The influence of air and sea exchange on the
 664 carbon isotope distribution in the sea. *Global Biogeochemical Cycles*, *6*(3), 315-320.
 665 doi:10.1029/92GB01672
- 666 Broecker, W. S., & Peng, T. H. (1982). *Tracers in the sea*. Lamont-Doherty Earth Observ.,
 667 Palisades, N. Y.
- 668 Corliss, B. H., Sun, X., Brown, C. W., & Showers, W. J. (2006). Influence of seasonal primary
 669 productivity on $\delta^{13}\text{C}$ of North Atlantic deep-sea benthic foraminifera. *Deep Sea Research*
 670 *Part I: Oceanographic Research Papers*, *53*(4), 740-746. doi:10.1016/j.dsr.2006.01.006
- 671 Curry, W. B., Duplessy, J. C., Labeyrie, L. D., & Shackleton, N. J. (1988). Changes in the
 672 distribution of $\delta^{13}\text{C}$ of deep water ΣCO_2 between the last glaciation and the Holocene.
 673 *Paleoceanography*, *3*(3), 317-341. doi:10.1029/PA003i003p00317
- 674 Devriendt, L. S., Watkins, J. M., & McGregor, H. V. (2017). Oxygen isotope fractionation in the
 675 $\text{CaCO}_3\text{-DIC-H}_2\text{O}$ system. *Geochimica et Cosmochimica Acta*, *214*, 115-142.
 676 doi:10.1016/j.gca.2017.06.022
- 677 Duplessy, J.-C., Labeyrie, L., & Waelbroeck, C. (2002). Constraints on the ocean oxygen
 678 isotopic enrichment between the Last Glacial Maximum and the Holocene:
 679 Paleoceanographic implications. *Quaternary Science Reviews*, *21*, 315-330.
 680 doi:10.1016/S0277-3791(01)00107-X
- 681 Duplessy, J.-C., Shackleton, N. J., Matthews, R. K., Prell, W., Ruddiman, W. F., Caralp, M., &
 682 Hendy, C. H. (1984). ^{13}C record of benthic foraminifera in the Last Interglacial ocean -
 683 implications for the carbon-cycle and the global deep-water circulation. *Quaternary*
 684 *Research*, *21*(2), 225-243. doi:10.1016/0033-5894(84)90099-1
- 685 Eide, M., Olsen, A., Ninnemann, U. S., & Johannessen, T. (2017). A global ocean climatology of
 686 preindustrial and modern ocean $\delta^{13}\text{C}$. *Global Biogeochemical Cycles*, *31*(3), 515-534.
 687 doi:10.1002/2016gb005473
- 688 Elderfield, H., Yu, J., Anand, P., Kiefer, T., & Nyland, B. (2006). Calibrations for benthic
 689 foraminiferal Mg/Ca paleothermometry and the carbonate ion hypothesis. *Earth and*
 690 *Planetary Science Letters*, *250*(3-4), 633-649. doi:10.1016/j.epsl.2006.07.041
- 691 Emerson, S., & Hedges, J. (2008). *Chemical oceanography and the marine carbon cycle*:
 692 Cambridge: Cambridge University Press. <https://doi.org/10.1017/CBO9780511793202>.
- 693 Emery, W. J. (2001). Water types and water masses. In J. H. Steele (Ed.), *Encyclopedia of Ocean*
 694 *Sciences, 1st Edition* (Vol. 6, pp. 3179-3187): Elsevier.

- 695 Erez, J. (2003). The source of ions for biomineralization in foraminifera and their implications
 696 for paleoceanographic proxies. *Reviews in Mineralogy and Geochemistry*, 54(1), 115-
 697 149. doi:10.2113/0540115
- 698 Farrar, D. E., & Glauber, R. R. (1967). Multicollinearity in regression analysis - Problem
 699 revisited. *Review of Economics and Statistics*, 49(1), 92-107. doi:10.2307/1937887
- 700 Gill, A. E. (1973). Circulation and bottom water production in Weddell Sea. *Deep-Sea Research*,
 701 20(2), 111-140. doi:10.1016/0011-7471(73)90048-X
- 702 Gillooly, J. F., Brown, J. H., West, G. B., Savage, V. M., & Charnov, E. L. (2001). Effects of
 703 size and temperature on metabolic rate. *Science*, 293(5538), 2248-2251.
 704 doi:10.1126/science.1061967
- 705 Gooday, A. J. (2002). Biological responses to seasonally varying fluxes of organic matter to the
 706 ocean floor: A review. *Journal of Oceanography*, 58(2), 305-332.
 707 doi:10.1023/A:1015865826379
- 708 Gottschalk, J., Vázquez Riveiros, N., Waelbroeck, C., Skinner, L. C., Michel, E., Duplessy, J.-
 709 C., et al. (2016). Carbon isotope offsets between benthic foraminifer species of the genus
 710 *Cibicides* (*Cibicidoides*) in the glacial sub-Antarctic Atlantic. *Paleoceanography*, 31(12),
 711 1583-1602. doi:10.1002/2016pa003029
- 712 Hesse, T., Butzin, M., Bickert, T., & Lohmann, G. (2011). A model-data comparison of $\delta^{13}\text{C}$ in
 713 the glacial Atlantic Ocean. *Paleoceanography*, 26. doi:10.1029/2010PA002085
- 714 Hesse, T., Wolf-Gladrow, D., Lohmann, G., Bijma, J., Mackensen, A., & Zeebe, R. E. (2014).
 715 Modelling $\delta^{13}\text{C}$ in benthic foraminifera: Insights from model sensitivity experiments.
 716 *Marine Micropaleontology*, 112, 50-61. doi:10.1016/j.marmicro.2014.08.001
- 717 Hodell, D. A., Venz, K. A., Charles, C. D., & Ninnemann, U. S. (2003). Pleistocene vertical
 718 carbon isotope and carbonate gradients in the South Atlantic sector of the Southern
 719 Ocean. *Geochemistry, Geophysics, Geosystems*, 4(1), 1-19. doi:10.1029/2002gc000367
- 720 Hodell, D. A., & Venz-Curtis, K. A. (2006). Late Neogene history of deepwater ventilation in
 721 the Southern Ocean. *Geochemistry, Geophysics, Geosystems*, 7(9), n/a-n/a.
 722 doi:10.1029/2005gc001211
- 723 Holbourn, A., Henderson, A. S., & Macleod, N. (2013). *Atlas of benthic foraminifera*.
 724 Chichester, U.K.: Wiley-Blackwell.
- 725 Jorissen, F. J., Wittling, I., Peypouquet, J. P., Rabouille, C., & Relexans, J. C. (1998). Live
 726 benthic foraminiferal faunas off Cape Blanc, NW-Africa: Community structure and
 727 microhabitats. *Deep-Sea Research Part I-Oceanographic Research Papers*, 45(12),
 728 2157-2188. doi:10.1016/S0967-0637(98)00056-9
- 729 Juranek, L. W., A. D. Russell, and H. J. Spero (2003), Seasonal oxygen and carbon isotope
 730 variability in euthecosomatous pteropods from the Sargasso Sea, *Deep-Sea Research I*,
 731 50(231-245). doi:10.1016/j.gca.2013.12.034
- 732 Key, R. M., Kozyr, A., Sabine, C. L., Lee, K., Wanninkhof, R., Bullister, J. L., et al. (2004). A
 733 global ocean carbon climatology: Results from Global Data Analysis Project (GLODAP).
 734 *Global Biogeochemical Cycles*, 18(4). doi:10.1029/2004gb002247

- 735 Kim, S. T., & O'Neil, J. R. (1997). Equilibrium and nonequilibrium oxygen isotope effects in
 736 synthetic carbonates. *Geochimica et Cosmochimica Acta*, *61*(16), 3461-3475.
 737 doi:10.1016/S0016-7037(97)00169-5
- 738 Krief, S., Hendy, E. J., Fine, M., Yam, R., Meibom, A., Foster, G. L., & Shemesh, A. (2010).
 739 Physiological and isotopic responses of scleractinian corals to ocean acidification.
 740 *Geochimica et Cosmochimica Acta*, *74*(17), 4988-5001. doi:10.1016/j.gca.2010.05.023
- 741 Lisiecki, L. E., & Raymo, M. E. (2005). A Pliocene-Pleistocene stack of 57 globally distributed
 742 benthic $\delta^{18}\text{O}$ records. *Paleoceanography*, *20*(1), PA1003. doi:10.1029/2004pa001071
- 743 Lutze, G. F., & Thiel, H. (1989). Epibenthic foraminifera from elevated microhabitats -
 744 *Cibicidoides wuellerstorfi* and *Planulina ariminensis*. *Journal of Foraminiferal Research*,
 745 *19*(2), 153-158. doi:10.2113/gsjfr.19.2.153
- 746 Mackensen, A. (2012). Strong thermodynamic imprint on Recent bottom-water and epibenthic
 747 delta $\delta^{13}\text{C}$ in the Weddell Sea revealed: Implications for glacial Southern Ocean
 748 ventilation. *Earth and Planetary Science Letters*, *317*, 20-26.
 749 doi:10.1016/j.epsl.2011.11.030
- 750 Mackensen, A., Hubberten, H. W., Bickert, T., Fischer, G., & Fütterer, D. K. (1993). The $\delta^{13}\text{C}$ in
 751 benthic foraminiferal tests of *Fontbotia wuellerstorfi* (Schwager) relative to the $\delta^{13}\text{C}$ of
 752 dissolved inorganic carbon in Southern-Ocean Deep-Water - Implications for glacial
 753 ocean circulation models. *Paleoceanography*, *8*(5), 587-610. doi:10.1029/93PA01291
- 754 Mackensen, A., Rudolph, M., & Kuhn, G. (2001). Late Pleistocene deep-water circulation in the
 755 subantarctic eastern Atlantic. *Global and Planetary Change*, *30*(3-4), 197-229.
 756 doi:10.1016/S0921-8181(01)00102-3
- 757 Marchitto, T. M., Curry, W. B., Lynch-Stieglitz, J., Bryan, S. P., Cobb, K. M., & Lund, D. C.
 758 (2014). Improved oxygen isotope temperature calibrations for cosmopolitan benthic
 759 foraminifera. *Geochimica et Cosmochimica Acta*, *130*, 1-11.
 760 doi:10.1016/j.gca.2013.12.034
- 761 Martin, J. H., Knauer, G. A., Karl, D. M., & Broenkow, W. W. (1987). VERTEX - carbon
 762 cycling in the northeast Pacific. *Deep-Sea Research Part a-Oceanographic Research*
 763 *Papers*, *34*(2), 267-285. doi:10.1016/0198-0149(87)90086-0
- 764 Matsumoto, K., & Lynch-Stieglitz, J. (1999). Similar glacial and Holocene deep water
 765 circulation inferred from southeast Pacific benthic foraminiferal carbon isotope
 766 composition. *Paleoceanography*, *14*(2), 149-163. doi:10.1029/1998pa900028
- 767 McConnaughey, T. (1989a). ^{13}C and ^{18}O isotopic disequilibrium in biological carbonates .1.
 768 Patterns. *Geochimica et Cosmochimica Acta*, *53*(1), 151-162. doi:10.1016/0016-
 769 7037(89)90282-2
- 770 McCorkle, D. C., Keigwin, L. D., Corliss, B. H., & Emerson, S. R. (1990). The influence of
 771 microhabitats on the carbon isotopic composition of deep-sea benthic foraminifera.
 772 *Paleoceanography*, *5*(2), 161-185. doi:10.1029/PA005i002p00161
- 773 Millero, F. J. (1995). Thermodynamics of the carbon dioxide System in the oceans. *Geochimica*
 774 *et Cosmochimica Acta*, *59*(4), 661-677. doi:10.1016/0016-7037(94)00354-O

- 775 Millero, F. J., Graham, T. B., Huang, F., Bustos-Serrano, H., & Pierrot, D. (2006). Dissociation
776 constants of carbonic acid in seawater as a function of salinity and temperature. *Marine*
777 *Chemistry*, 100(1-2), 80-94. doi:10.1016/j.marchem.2005.12.001
- 778 Moodley, L., Middelburg, J. J., Soetaert, K., Boschker, H. T. S., Herman, P. M. J., & Heip, C. H.
779 R. (2005). Similar rapid response to phytodetritus deposition in shallow and deep-sea
780 sediments. *Journal of Marine Research*, 63(2), 457-469. doi:10.1357/0022240053693662
- 781 Mook, W. G. (2000). Environmental Isotopes in the Hydrological Cycle: Principles and
782 Applications. Vol 1: Introduction, Theory, Methods, Review. In Technical Documents in
783 Hydrology No. 39: IAEA - UNESCO.
- 784 Nederbragt, A. J. (2023): $\delta^{18}\text{O}$ and $\delta^{13}\text{C}$ of *Cibicidoides wuellerstorfi* and related species and
785 carbonate chemistry of ambient sea water [Dataset]. *PANGAEA*,
786 <https://doi.org/10.1594/PANGAEA.960367>
- 787 Nimon, K. F., & Oswald, F. L. (2013). Understanding the results of multiple linear regression:
788 Beyond standardized regression coefficients. *Organizational Research Methods*, 16(4),
789 650-674. doi:10.1177/1094428113493929
- 790 Ninnemann, U. S., & Charles, C. D. (2002). Changes in the mode of Southern Ocean circulation
791 over the last glacial cycle revealed by foraminiferal stable isotopic variability. *Earth and*
792 *Planetary Science Letters*, 201(2), 383-396. doi:10.1016/S0012-821X(02)00708-2
- 793 Peterson, C. D., Lisiecki, L. E., & Stern, J. V. (2014). Deglacial whole-ocean $\delta^{13}\text{C}$ change
794 estimated from 480 benthic foraminiferal records. *Paleoceanography*, 29(6), 549-563.
795 doi:10.1002/2013pa002552
- 796 Romanek, C. S., Grossman, E. L., & Morse, J. W. (1992). Carbon isotopic fractionation in
797 synthetic aragonite and calcite - effects of temperature and precipitation rate. *Geochimica*
798 *et Cosmochimica Acta*, 56(1), 419-430. doi:10.1016/0016-7037(92)90142-6
- 799 Schmidt, G. A. (1999). Forward modeling of carbonate proxy data from planktonic foraminifera
800 using oxygen isotope tracers in a global ocean model. *Paleoceanography*, 14(4), 482-497
801 (Schmidt, G.A., Bigg, G.R., Rohling, E.J., 1999. Global Seawater Oxygen-18 Database.
802 (<http://data.giss.nasa.gov/o18data/>).). doi:10.1029/1999PA900025
- 803 Schmittner, A., Bostock, H. C., Cartapanis, O., Curry, W. B., Filipsson, H. L., Galbraith, E. D.,
804 et al. (2017). Calibration of the carbon isotope composition ($\delta^{13}\text{C}$) of benthic
805 foraminifera. *Paleoceanography*, 32(6), 512-530. doi:10.1002/2016PA003072
- 806 Schweizer, M. (2006). *Evolution and molecular phylogeny of Cibicides and Uvigerina*
807 (*Rotaliida, Foraminifera*) (Vol. 261).
- 808 Sigman, D. M., Hain, M. P., & Haug, G. H. (2010). The polar ocean and glacial cycles in
809 atmospheric CO_2 concentration. *Nature*, 466(7302), 47-55. doi:10.1038/nature09149
- 810 Sokal, R. R., & Rohlf, F. J. (1994). *Biometry: Principles and practice of statistics in biological*
811 *research (3rd edition)*. San Francisco: W.H. Freeman.
- 812 Spero, H. J., Bijma, J., Lea, D. W., & Bemis, B. E. (1997). Effect of seawater carbonate
813 concentration on foraminiferal carbon and oxygen isotopes. *Nature*, 390(6659), 497-500.
814 doi:10.1038/37333

- 815 Sundquist, E. T. (1993). The global carbon dioxide budget. *Science*, 259(5097), 934-941.
816 doi:10.1126/science.259.5097.934
- 817 Talley, L. D., Pickard, G. L., Emery, W. J., & Swift, J. H. (2011). *Descriptive physical*
818 *oceanography (6th edition) - An introduction*: Academic Press.
- 819 Watkins, J. M., Hunt, J. D., Ryerson, F. J., & DePaolo, D. J. (2014). The influence of
820 temperature, pH, and growth rate on the $\delta^{18}\text{O}$ composition of inorganically precipitated
821 calcite. *Earth and Planetary Science Letters*, 404, 332-343.
822 doi:10.1016/j.epsl.2014.07.036
- 823 Wollenburg, J. E., Zittier, Z. M. C., & Bijma, J. (2018). Insight into deep-sea life – *Cibicidoides*
824 *pachyderma* substrate and pH-dependent behaviour following disturbance. *Deep Sea*
825 *Research Part I: Oceanographic Research Papers*, 138, 34-45.
826 doi:10.1016/j.dsr.2018.07.006
- 827 Yu, J., & Elderfield, H. (2007). Benthic foraminiferal B/Ca ratios reflect deep water carbonate
828 saturation state. *Earth and Planetary Science Letters*, 258(1-2), 73-86.
829 doi:10.1016/j.epsl.2007.03.025
- 830 Yu, J. M., Anderson, R. F., Jin, Z. D., Rae, J. W. B., Opdyke, B. N., & Eggins, S. M. (2013).
831 Responses of the deep ocean carbonate system to carbon reorganization during the Last
832 Glacial-interglacial cycle. *Quaternary Science Reviews*, 76, 39-52.
833 doi:10.1016/j.quascirev.2013.06.020
- 834 Yu, J. M., Elderfield, H., & Honisch, B. (2007). B/Ca in planktonic foraminifera as a proxy for
835 surface seawater pH. *Paleoceanography*, 22(2). doi:10.1029/2006PA001347
- 836 Yu, J., et al. (2016), Sequestration of carbon in the deep Atlantic during the last glaciation,
837 *Nature Geoscience*, 9(4), 319-+. doi:10.1038/NGEO2657
- 838 Zahn, R., Winn, K., & Samthein, M. (1986). Benthic foraminiferal $\delta^{13}\text{C}$ and accumulation rates
839 of organic carbon: *Uvigerina peregrina* group and *Cibicidoides wuellerstorfi*.
840 *Paleoceanography*, 1(1), 27-42. doi:10.1029/PA001i001p00027
- 841 Zeebe, R. E. (1999). An explanation of the effect of seawater carbonate concentration on
842 foraminiferal oxygen isotopes. *Geochimica et Cosmochimica Acta*, 63(13-14), 2001-
843 2007. doi:10.1016/S0016-7037(99)00091-5
- 844 Zeebe, R. E., Bijma, J., & Wolf-Gladrow, D. A. (1999). A diffusion-reaction model of carbon
845 isotope fractionation in foraminifera. *Marine Chemistry*, 64(3), 199-227.
846 doi:10.1016/S0304-4203(98)00075-9
- 847 Ziveri, P., Thoms, S., Probert, I., Geisen, M., & Langer, G. (2012). A universal carbonate ion
848 effect on stable oxygen isotope ratios in unicellular planktonic calcifying organisms.
849 *Biogeosciences*, 9(3), 1025-1032. doi:10.5194/bg-9-1025-2012
- 850 Zuddas, P., & Mucci, A. (1994). Kinetics of calcite precipitation from seawater: I. A classical
851 chemical kinetics description for strong electrolyte solutions. *Geochimica et*
852 *Cosmochimica Acta*, 58(20), 4353-4362. doi:10.1016/0016-7037(94)90339-5
- 853

854

855 **Table 1.** Selected bivariate correlation coefficients for $\Delta^{13}\text{C}_{\text{Cwue}}$, $\Delta^{18}\text{O}_{\text{Cwue}}$, and oceanographic
 856 variables; ns indicates the correlation is not significantly different from $r=0$ at the 99%
 857 confidence level.

858

	$\Delta^{13}\text{C}_{\text{Cwue}}$			$\Delta^{18}\text{O}_{\text{Cwue}}$			Depth	T	DIC	pH
	all	nAtl	nIPac	all	nAtl	nIPac				
n	252	122	76	252	122	76	252	252	252	252
Depth	-0.47	-0.52	-0.48	-0.38	-0.61	ns	-	-0.69	ns	ns
T	0.33	0.56	0.41	ns	0.54	ns	-0.69	-	-0.49	0.42
S	-0.19	0.45	ns	-0.31	0.40	ns	ns	0.28	-0.58	0.63
Ω_{cal}	0.20	0.49	0.47	ns	0.58	ns	-0.78	0.84	-0.65	0.69
$\Delta[\text{CO}_3^{2-}]$	0.19	0.47	0.46	ns	0.52	ns	-0.77	0.76	-0.65	0.73
DIC	0.33	ns	ns	0.28	ns	ns	ns	-0.49	-	-0.94
TA	0.26	ns	ns	ns	-0.44	ns	0.33	-0.56	0.95	-0.82
pH	-0.27	ns	ns	-0.30	ns	ns	ns	0.42	-0.94	-
$[\text{HCO}_3^-]$	0.32	ns	ns	0.29	ns	ns	ns	-0.50	1.00	-0.95
$[\text{CO}_3^{2-}]$	-0.30	ns	ns	-0.37	ns	ns	ns	0.41	-0.92	0.96
$[\text{CO}_2]_{\text{aq}}$	0.43	0.29	ns	0.41	ns	ns	-0.24	-0.22	0.89	-0.91
$f\text{CO}_2$	0.51	0.42	0.34	0.45	0.44	ns	-0.39	ns	0.79	-0.84

859

860

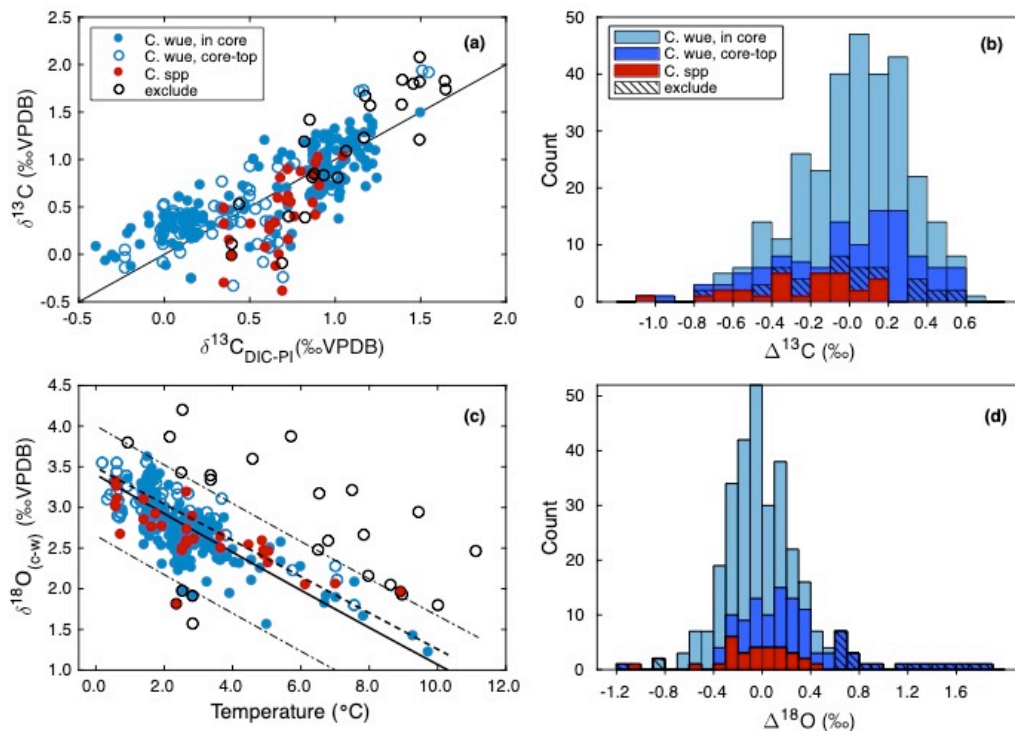
861 **Table 2.** Shift in $\Delta^{13}\text{C}_{\text{Cwue}}$ and $\Delta^{18}\text{O}_{\text{Cwue}}$ between LGM-LH expected from Eqs 3-6 and published
 862 estimates for ocean temperature (Adkins et al., 2002; Duplessy et al., 2002), [DIC] (Sundquist,
 863 1993), and $\Delta[\text{CO}_3^{2-}]$ (Anderson & Archer, 2002; Yu et al., 2013).

864

	Pacific					Atlantic (deep)				
	LGM-LH	$\Delta^{13}\text{C}$ (‰)			$\Delta^{18}\text{O}$ (‰)	LGM-LH	$\Delta^{13}\text{C}$ (‰)			$\Delta^{18}\text{O}$ (‰)
		eq. 3	eq. 4	eq. 5	eq. 6		eq. 3	eq. 4	eq. 5	eq. 6
ΔDIC	45 $\mu\text{mol/kg}$	0.12	0.14	0.14	0.09	45 $\mu\text{mol/kg}$	0.12	0.14	0.14	0.09
ΔT	-2.5°C	-0.30	-	-0.20	-	-3.5°C	-0.43	-	-0.28	-
$\Delta[\text{CO}_3^{2-}]$	0 $\mu\text{mol/kg}$	-	0.00	0.00	0.00	-20 $\mu\text{mol/kg}$	-	-0.16	-0.08	-0.09
total		-0.19	0.14	-0.06	0.09		-0.31	-0.02	-0.22	0.00

865

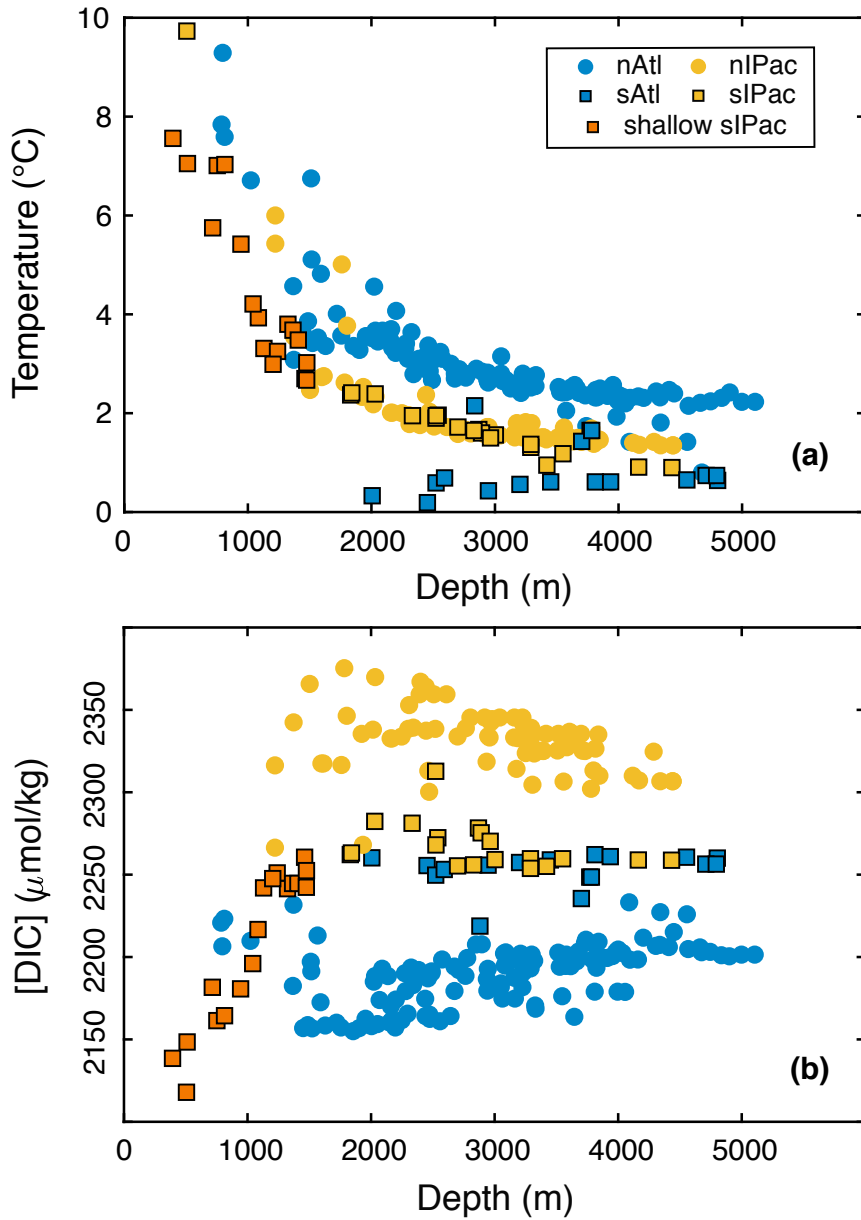
866 **Figure 1.** (a) Plot of $\delta^{13}\text{C}$ of *C. wuellerstorfi* and *Cibicidoides* spp against $\delta^{13}\text{C}_{\text{DIC-PI}}$, black line
 867 denotes the 1:1 relationship. Black circles denote data that are excluded based on outlying $\delta^{18}\text{O}$
 868 values as shown in (c); (b) Histogram of $\Delta^{13}\text{C}$ for data in (a); (c) Plot of $\delta^{18}\text{O}_{(\text{c-w})}$ against
 869 temperature with symbols as in (a), the subscript (c-w) refers to the measured value corrected for
 870 ambient $\delta^{18}\text{O}_{\text{water}}$. Black line indicates expected values based on the temperature equation of Kim
 871 & O'Neil (1997) as adjusted by Bohm et al. (2000), dashed line represents the empirical
 872 temperature equation for *Cibicidoides* spp (Marchitto et al., 2014). Dash-dot lines represent cut-
 873 off levels used to define outliers; (d) Histogram of $\Delta^{18}\text{O}$ for data in (c) with symbols as in (b).
 874 For further description see section 3.1.



875

876

877 **Figure 2.** (a) Temperature and (b) [DIC] for all *C. wuellerstorfi* localities plotted against water
 878 depth, to illustrate differences between core localities grouped by ocean region; for further
 879 description see section 2.2.



881 **Figure 3.** Correlation between $\Delta^{18}\text{O}$ and $\Delta^{13}\text{C}$. (a) Cross plot of $\Delta^{18}\text{O}$ against $\Delta^{13}\text{C}$ for all
 882 *Cibicidoides* data; black and red lines represent orthogonal regression lines for *C. wuellerstorfi*
 883 and *Cibicidoides* spp respectively; (b) and (c) show cross plots of $\Delta^{13}\text{C}$ and $\Delta^{18}\text{O}$ data
 884 respectively paired *Cibicidoides* spp and *C. wuellerstorfi* data; black lines indicate the 1:1
 885 relationship; (d) and (e) show the standard deviation (s) for $\Delta^{13}\text{C}_{\text{Cwue}}$ and $\Delta^{18}\text{O}_{\text{Cwue}}$ respectively
 886 for multiple analyses ($n \geq 3$) from a single locality. Note that for $\Delta^{13}\text{C}$ the between-sample
 887 variability increases as $\Delta^{13}\text{C}_{\text{Cwue}}$ decreases, while the variability of $\Delta^{18}\text{O}_{\text{Cwue}}$ is independent of the
 888 measured value.

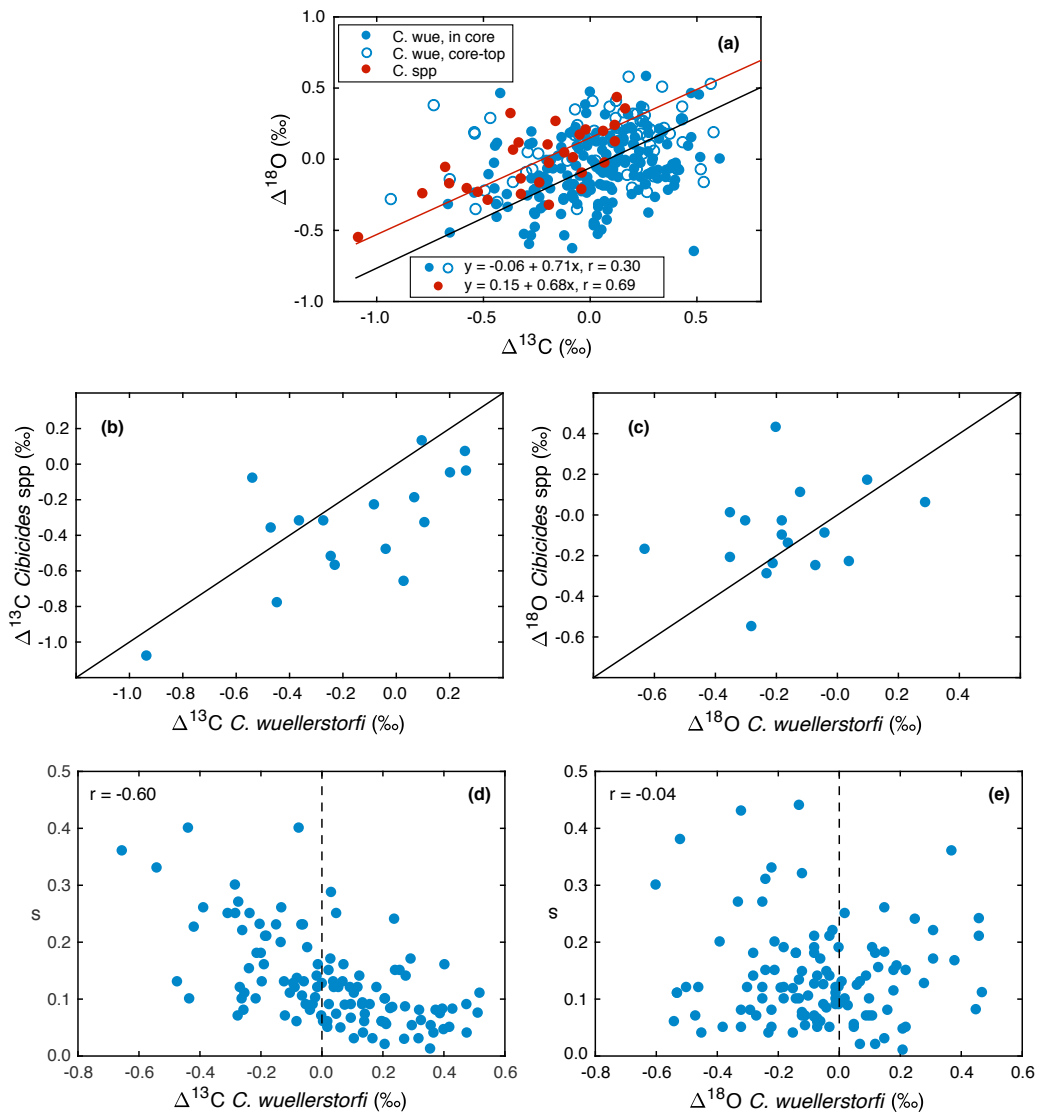


Figure 3

889

890

891 **Figure 4.** Plots of $\Delta^{13}\text{C}_{\text{Cwue}}$ against selected oceanographic variables with data separated by
 892 ocean region as shown in Fig. 2. Black lines represent regression lines for Atlantic (i) and Indo-
 893 Pacific data (ii) separately, dashed lines indicate that the correlation is not significant at the 99%
 894 confidence level.

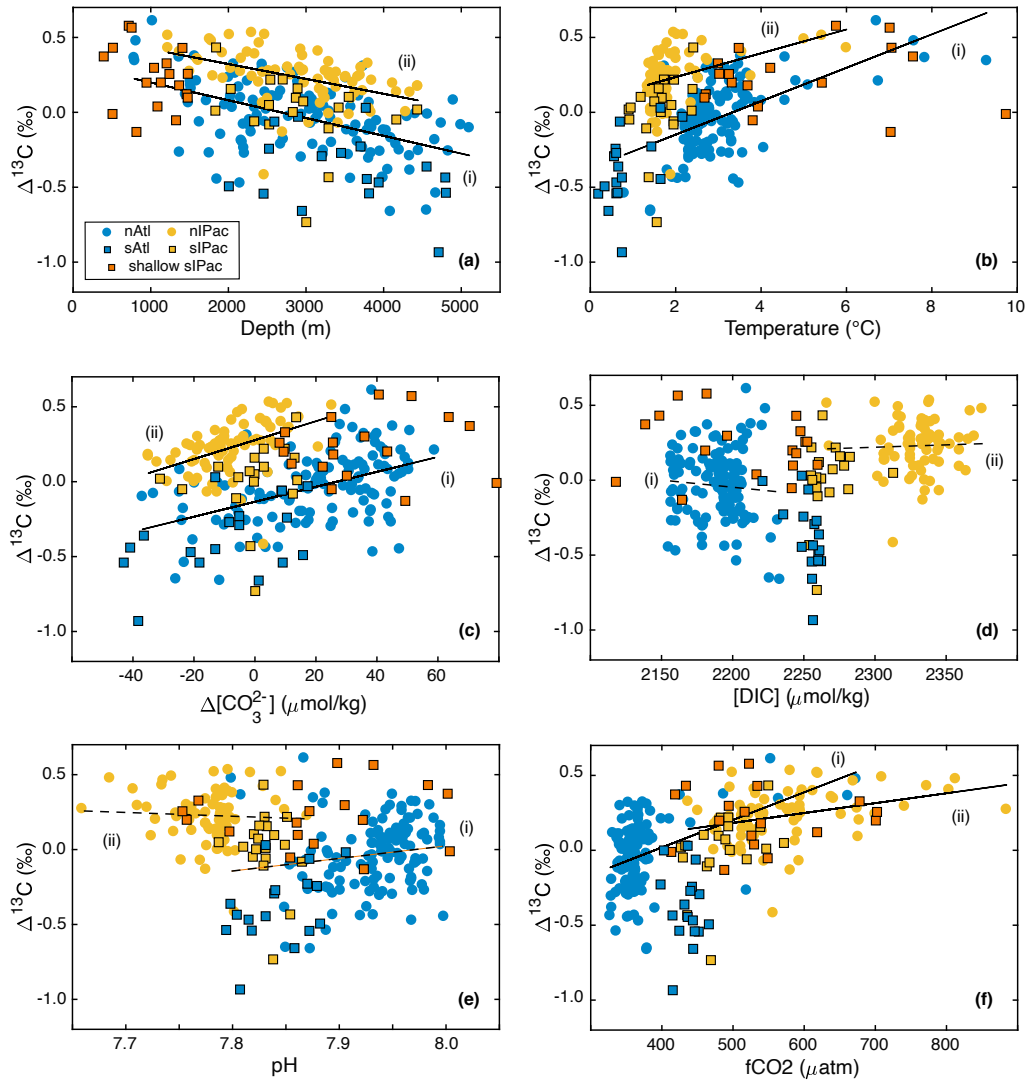


Figure 4

895

896

897 **Figure 5.** Contour plots of $\Delta^{13}\text{C}_{\text{Cwue}}$ to illustrate multilinear relation with oceanographic
 898 conditions. (a) scatter plot of temperature and [DIC] showing distribution of data points, and (b)
 899 contour plot of $\Delta^{13}\text{C}_{\text{Cwue}}$ as a function of temperature and [DIC], thick lines indicate iso-plane
 900 described by equation 4; (c) scatter plot as in (a) but for $\Delta[\text{CO}_3^{2-}]$ and [DIC] and (d) contour plot
 901 of $\Delta^{13}\text{C}_{\text{Cwue}}$ against $\Delta[\text{CO}_3^{2-}]$ and [DIC] with lines calculated from equation 5.

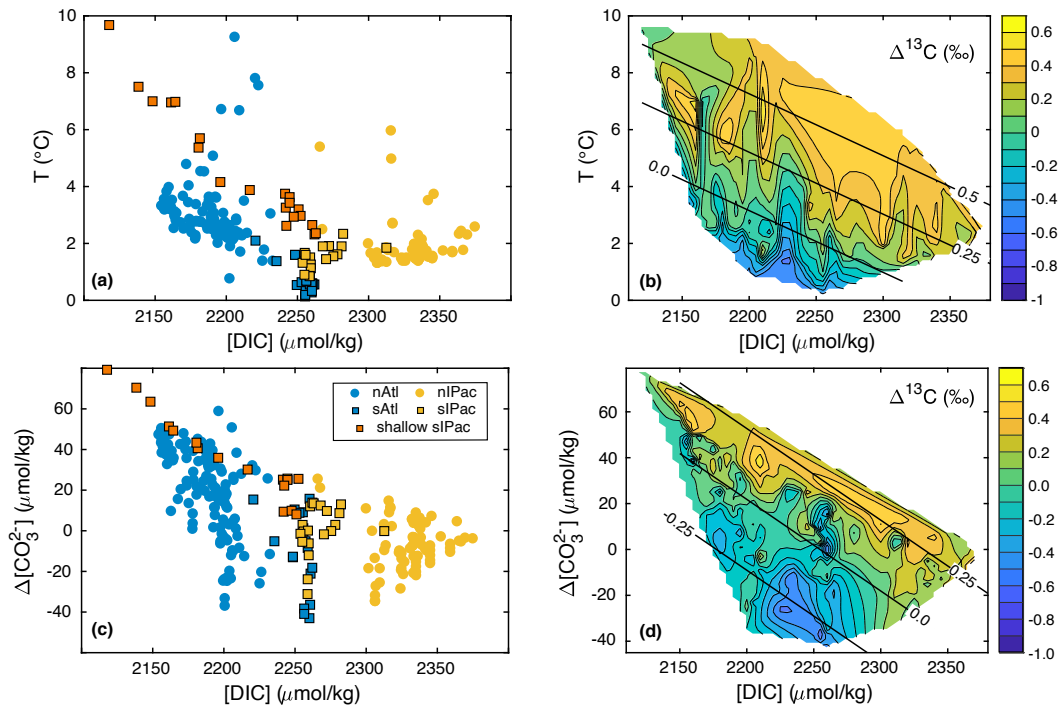
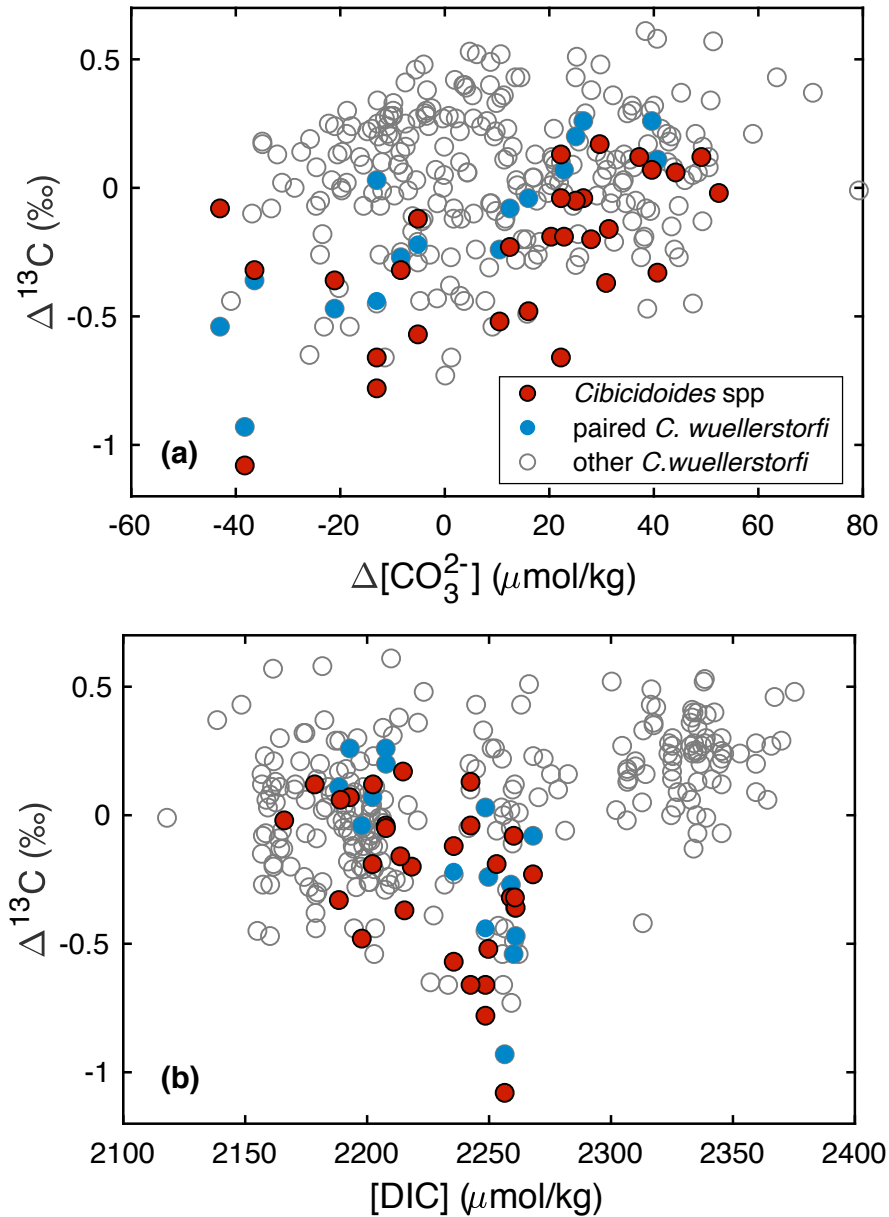


Figure 5

902

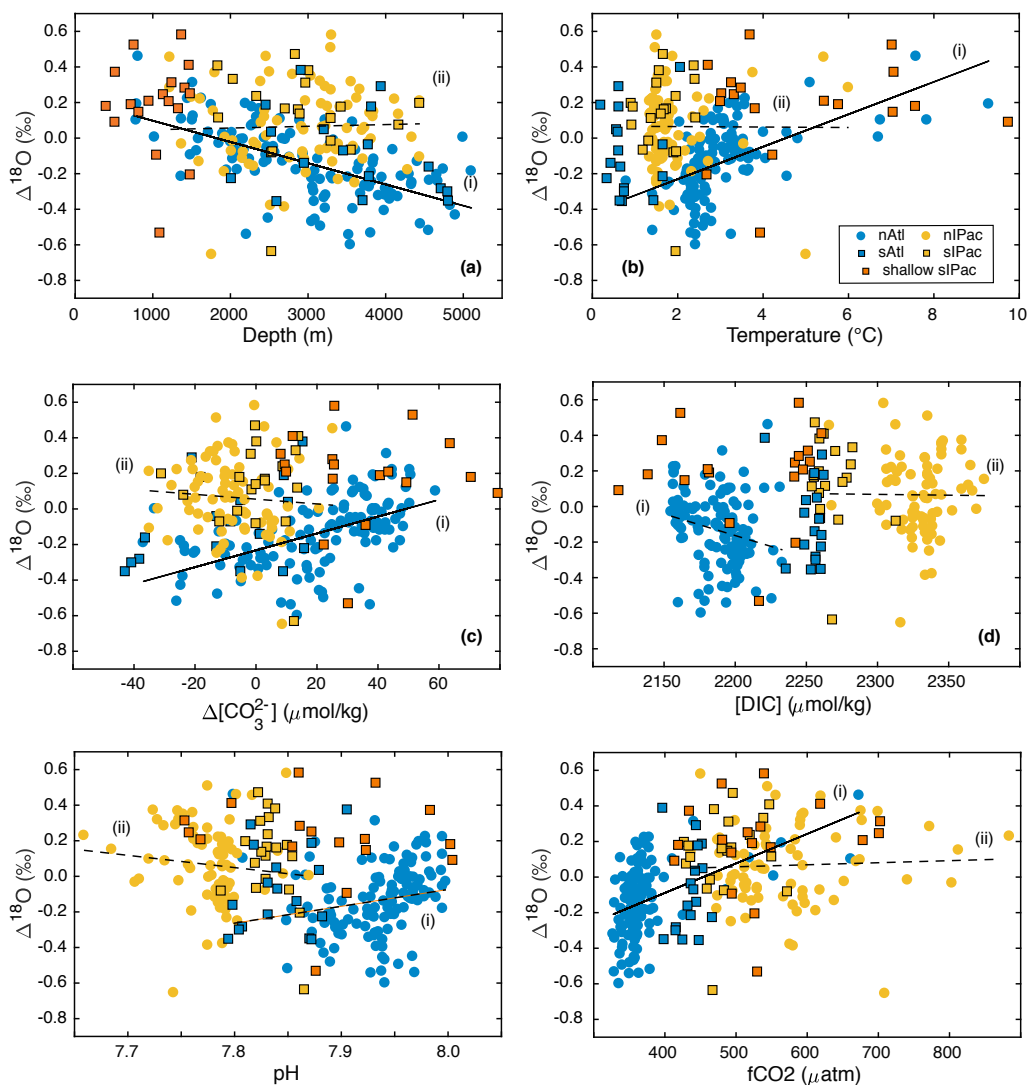
903

904 **Figure 6.** Scatter plot of $\Delta^{13}\text{C}_{\text{Csp}}^{\text{spp}}$ against (a) $\Delta[\text{CO}_3^{2-}]$ and (b) [DIC] with data for *C.*
 905 *wuellerstorfi* shown for comparison. Note that $\Delta^{13}\text{C}_{\text{Csp}}^{\text{spp}}$ is lower on average than $\Delta^{13}\text{C}_{\text{Cwue}}$ from
 906 the same core as shown in Fig. 3B.



908 **Supplementary Tables and Figures**

909 **Figure S1.** Plots of $\Delta^{18}\text{O}_{\text{C}_{\text{wue}}}$ against selected oceanographic variables with data split by ocean
 910 region. Black lines represent regression lines for Atlantic (i) and Indo-Pacific data (ii) separately,
 911 dashed lines indicate that the correlation is not significant at the 99% confidence level. Note that
 912 the distribution pattern of $\Delta^{18}\text{O}_{\text{C}_{\text{wue}}}$ with all variables is similar to that of $\Delta^{13}\text{C}_{\text{C}_{\text{wue}}}$ but that
 913 correlation coefficients are consistently weaker.



914

915

916 **Table S1.** Amount of variation explained by multiple linear regression of $\Delta^{13}\text{C}_{\text{Cwue}}$ and $\Delta^{18}\text{O}_{\text{Cwue}}$
 917 against pairs of two independent variables. Bold values indicate $R^2 > 0.35$ for $\Delta^{13}\text{C}_{\text{Cwue}}$ and $R^2 >$
 918 0.25 for $\Delta^{18}\text{O}_{\text{Cwue}}$; ns indicates values that are not significant at the 99% confidence level.

919

$\Delta^{13}\text{C}$	T	S	Depth	DIC	TA	pH	$[\text{HCO}_3^-]$	$[\text{CO}_3^{=}]$	$[\text{CO}_2]_{\text{aq}}$	fCO ₂	Ω_{cal}	$\Delta[\text{CO}_3^{=}]$
T	-											
S	0.200	-										
Depth	0.219	0.239	-									
DIC	0.426	0.109	0.372	-								
TA	0.397	0.075	0.407	0.137	-							
pH	0.309	0.072	0.335	0.124	0.075	-						
$[\text{HCO}_3^-]$	0.418	0.100	0.361	0.161	0.111	0.112	-					
$[\text{CO}_3^{=}]$	0.335	0.090	0.298	0.109	0.091	0.094	0.100	-				
$[\text{CO}_2]_{\text{aq}}$	0.374	0.199	0.326	0.195	0.187	0.276	0.207	0.345	-			
fCO ₂	0.370	0.283	0.346	0.276	0.263	0.354	0.285	0.384	0.353	-		
Ω_{cal}	0.133	0.108	0.293	0.399	0.349	0.344	0.389	0.287	0.341	0.361	-	
$\Delta[\text{CO}_3^{=}]$	0.119	0.117	0.294	0.391	0.322	0.383	0.384	0.294	0.342	0.369	0.038	-

$\Delta^{18}\text{O}$	T	S	Depth	DIC	TA	pH	$[\text{HCO}_3^-]$	$[\text{CO}_3^{=}]$	$[\text{CO}_2]_{\text{aq}}$	fCO ₂	Ω_{cal}	$\Delta[\text{CO}_3^{=}]$
T	-											
S	0.158	-										
Depth	0.171	0.219	-									
DIC	0.187	0.114	0.257	-								
TA	0.099	0.099	0.229	0.214	-							
pH	0.176	0.114	0.272	0.087	0.113	-						
$[\text{HCO}_3^-]$	0.198	0.115	0.262	0.103	0.197	0.088	-					
$[\text{CO}_3^{=}]$	0.243	0.141	0.272	0.155	0.171	0.183	0.159	-				
$[\text{CO}_2]_{\text{aq}}$	0.231	0.174	0.256	0.203	0.209	0.211	0.203	0.181	-			
fCO ₂	0.224	0.205	0.252	0.217	0.222	0.227	0.216	0.208	0.214	-		
Ω_{cal}	n.s.	0.148	0.226	0.241	0.124	0.287	0.258	0.300	0.266	0.254	-	
$\Delta[\text{CO}_3^{=}]$	n.s.	0.140	0.270	0.194	0.080	0.262	0.211	0.266	0.240	0.239	0.047	-

920

921